Report
P-16-09
December 2018

Screening of radionuclides for radionuclide and dose calculations

Report for the safety evaluation SE-SFL

James Crawford

SVENSK KÄRNBRÄNSLEHANTERING AB

SWEDISH NUCLEAR FUEL
AND WASTE MANAGEMENT CO

Box 3091, SE-169 03 Solna
Phone +46 8 459 84 00
skb.se

SVENSK KÄRNBRÄNSLEHANTERING

ISSN 1651-4416
SKB P-16-09
ID 1606860
December 2018

Screening of radionuclides for radionuclide and dose calculations

Report for the safety evaluation SE-SFL

James Crawford
Kemakta Konsult AB

Keywords: SE-SFL, Prioritised radionuclides, Transport modelling.

Abstract

This report summarises scoping calculations made to determine a list of prioritised radionuclides for inclusion in the safety evaluation of a proposed repository concept for the repository for long-lived waste (SFL) for low and intermediate level waste. An evaluation has been made of the relative contributions to ingestion radiotoxicity for the different waste streams categorised as metallic wastes from the nuclear power plants (planned to be deposited in the BHK vault) and wastes from medicine, industry and research as well as legacy wastes (planned to be deposited in the BHA vault). A separate preliminary evaluation has also been made for radionuclide wastes deriving from the planned European Spallation Source (ESS) in Lund. Calculations have considered both the time evolution of the total waste inventory as well as migration screening calculations assuming a near-field source term provided by SKB.

Sammanfattning

Denna rapport sammanfattar överslagsberäkningar som har gjorts för att erhålla en lista över prioriterade radionuklider inför säkerhetsvärderingen av ett föreslaget förvarskoncept för slutförvaret för långlivat avfall (SFL) för låg och medelaktivt avfall. En uppskattning har tagits fram av de relativa bidragen till radiotoxicitet för de olika avfallsströmmar som har indelats som metalliskt avfall från kärnkraftverken (som planeras att deponeras i förvarssalen för härdkomponenter, BHK) och avfall från sjukvård, industri och forskning samt historiskt avfall (som planeras att deponeras i förvarssalen för historiskt avfall, BHA). En separat och preliminär beräkning har också gjorts för radioaktivt avfall från den planerade European Spallation Source (ESS) i Lund. Beräkningarna har beaktat både tidsutvecklingen av den totala radiotoxiciteten för samtliga avfallsströmmar samt en uppskattning av migrationspotentialen för radiotoxiciteten med hjälp av transportberäkningar med en förenklad källterm.

Contents

1 Introduction

The repository for long-lived waste (SFL) will be used for the final disposal of long-lived low and intermediate level waste from Swedish nuclear facilities. The waste to be deposited in SFL comprises waste from the operation and decommissioning of the Swedish nuclear power plants, legacy waste from early research in the Swedish nuclear programmes, and waste from medicine, industry and research. According to the proposed concept (Elfwing et al. 2013) evaluated in the safety evaluation SE-SFL, SFL is designed as a deep geological repository with two different sections:

- one section for metallic waste from the nuclear power plants designed with a concrete barrier, BHK, and
- one section for the waste from SNAB and AB SVAFO designed with a bentonite barrier, BHA.

In this report, the waste materials from the nuclear power plants are referred to as reactor waste and the waste materials to be deposited in BHA is referred to as legacy waste. A preliminary account of additional materials derived from the planned European Spallation Source (ESS) in Lund is also included in this report.

As the waste materials arise from a diverse range of sources, the radionuclide inventory also reflects this compositional diversity. Screening calculations to identify the most important dose contributors for geosphere migration calculations in an assessment of post-closure safety therefore fulfils two primary purposes:

1. Geosphere migration calculations are computationally demanding. Selection of prioritised nuclides identifies which contribute in a meaningful way to far-field transported radiotoxicity and which nuclides can be eliminated from dose calculations on the basis that they contribute negligibly.
2. Release boundary conditions and geosphere retardation parameters frequently have large uncertainty bounds. Selection of prioritised nuclides can assist in identifying which nuclides and sub-processes benefit most from extra attention during data compilation to lower uncertainty bounds on calculated biosphere dose rates.

Further to item 1) above, it can be added that the list of most important dose contributor's changes over time as some radionuclides decay to insignificance while others increase due to ingrowth. Calculations therefore need to consider a range of different time scales and possible release scenarios in order to properly screen for dose contribution so that important nuclides are not neglected.

In recent safety assessments for the Spent Fuel Repository, e.g. SR-Site (SKB 2010a), nuclides have been typically divided into several groups. These have included: 1) those that are important in all scenarios, 2) less important nuclides that may still be important in scenarios involving fast release (e.g. direct intrusion), 3) nuclides that only need to be characterised in terms of inventory and half-life (necessary for calculation of daughter nuclide inventory), and 4) those that can be excluded entirely. In the latest assessment of post-closure safety for the final repository for short-lived radioactive waste, SFR (SR-PSU; SKB 2014), on the other hand, nuclides were divided simply into: 1) those included in the inventory but not in the assessment, 2) nuclides explicitly included in both the inventory and the assessment, and 3) nuclides not included in the inventory but included as progeny in the assessment.

This report details screening calculations that have been made in support of identifying a set of radionuclides to be given priority status and which nuclides can be either neglected or relegated to the subgroups listed above for dose calculations in the safety evaluation SE-SFL.

2 Procedures adopted in previous safety assessments

In the radionuclide selection procedure adopted for SR-Site (SKB 2010a Appendix D) and SR-PSU (SKB 2015) non-chain nuclides having a half-life less than 10 y were excluded directly as well as those with a total inventory ingestion radiotoxicity less than 0.1 Sv. For the purposes of radionuclide transport calculations in SR-PSU, progeny with half-lives shorter than 100 days were assumed to be in equilibrium with their parent nuclide and excluded from migration calculations, although included implicitly in the landscape dose factor for the parent nuclide. Progeny with half-lives greater than 100 days although less than 1 year were explicitly modelled in transport calculations, although excluded from inventory calculations. Parent nuclides with short half-lives near the start of decay chains were also neglected by assuming rapid conversion to their progeny nuclides. Nuclides at the start of decay chains without any inventory could be excluded directly since they obviously cannot form by ingrowth.

In the SAR-08 safety assessment for SFR, screening calculations were made based on simplified transport calculations assuming equilibrium sorptive retardation along a representative 1D migration path and site-specific biosphere dose factors (Thomson et al. 2008). The screening dose was calculated with consideration given to equilibrium retarded travel time and decay for a specified advective travel time and migration path length while ingrowth of progeny nuclides was neglected. Apart from the inclusion of transport retardation effects, the main difference between the screening calculations made in SAR-08 relative to SR-Site and SR-PSU is that the screening was based on equivalent radiotoxicity flux (Sv/y) in SAR-08 rather than total inventory radiotoxicity (Sv). It is noted that the calculation of a radiotoxicity flux implies the assumption of a source term boundary condition, which in the case of SAR-08 was simply assumed to be proportional to the inventory radiotoxicity without consideration given to source depletion due to transport, solubility limitations, etc.

Another key difference is that the dose conversion factors used in the SR-Site and SR-PSU screening were ingestion dose coefficients taken from EU (1996), whereas in the SAR-08 screening calculations landscape dose factors were estimated for different representative ecosystem types relevant for the future state of the repository site.

3 Outline of screening calculations adopted in this work

In this work we have adopted a multi-level screening procedure whereby the inventory of radionuclides is tracked over time and assessed with regard to:

1. The equivalent radiotoxicity of individual radionuclides (radiotoxic inventory) existing in the waste materials as a function of time;
2. The relative far-field dose contributions of radionuclides transported along representative migration paths to the biosphere assuming a near-field release boundary condition supplied by SKB.

For the above, equivalent doses were calculated from activities using ingestion dose coefficients (and inhalation dose factors for gases) provided by SKB in the form of an MS Excel file based on ICRP (1995) and are the same values to be used in the SE-SFL radionuclide transport calculations.

In previous screening of radionuclides for safety assessment undertaken by Kemakta Konsult AB, the evolution of radionuclide inventory over time was calculated using an in-house developed program called DECAY. This program was based on numerical integration of the coupled first order ordinary differential equations describing radionuclide decay implemented in a Microsoft Excel macro linked to an external Fortran program. Recently, we have developed a new code family (NuDec) implemented in Matlab for simplified scoping calculations of radionuclide decay inventories, source terms, and far-field migration processes. The NuDec-Inventory program calculates the time evolution of radionuclide inventories using the matrix algebraic solution described by Moral and Pacheco (2003). The implementation of the algebraic solution algorithm in Matlab is advantageous as it allows additional pre- and post-processing operations to be performed for specific safety assessment screening tasks and can easily accommodate converging and diverging chains. The NuDec-Inventory modelling tool is described in more detail in Appendix A.

In this work, NuDec-Inventory is used to calculate the radiotoxicity inventory over time as an aid to first screening of priority radionuclides while the NuDec-Farf31 interface is used to calculate relative far-field dose contributions using the Farf31 performance assessment code (Norman and Kjellbert 1990, Lindgren et al. 2002) given a predefined source term. The source term flux for the transport screening calculations is described further in Chapter 5.

3.1 Input data for calculations

Radionuclide inventory data were supplied by SKB in the form of Microsoft Excel files. The data delivery contained induced radioactivity and surface contamination activity for the Barsebäck, Forsmark, Oskarshamn, Ringhals, and Ågesta reactors as documented in Herschend (2014) planned for disposal in BHK, as well as legacy waste materials originating from the Studsvik site planned for disposal in BHA[1].

Since the plans for the construction and operation of the European Spallation Source, ESS, are not yet finalised, only limited information is available concerning amount and composition of the waste from ESS. These data were not supplied in the form of spreadsheet files but were transcribed directly by the author of this report from tabulated values in a technical report[2]. Owing to the uncertainty associated with the inventory data from the ESS and the fact that several novel nuclides occur in the inventory (not all of which have ICRP defined dose conversion factors), the discussion of this waste stream has been handled separately to the BHA and BHK waste materials.

[1] Herschend B, 2015. Long-lived waste from AB SVAFO and Studsvik Nuclear AB. SKBdoc 1431282 ver 1.0, Svensk Kärnbränslehantering AB. (SKB internal document.)

[2] Persson P, 2018. Characteristics of radioactive waste from ESS to be disposed in SKB facilities. Technical Report, Document number ESS-0036701, Revision 2(3), SKBdoc 1701742 ver 1.0, Svensk Kärnbränslehantering AB.

Radionuclide decay constants were the same as those used previously in SR-PSU (SKB 2014, Table 3-4) which are predominantly taken from Firestone et al. (1999) with the exception of updated values for Ag-108m and Se-79 which were taken from Schrader (2004) and Jörg et al. (2010), respectively. Some decay constants were also taken from ICRP (2008) for new nuclides not included in previous safety assessments.

As mentioned previously, ingestion dose factors (Sv/Bq) for scoping calculation purposes are taken from ICRP (1995). Some fission and activation products belong to short (non-actinide) decay chains with one, or more progeny. In most cases the progeny nuclides have very short half-lives and their dose impact can be included in the dose of the parent nuclide (e.g. decay of Sr-90 to Y-90) by assuming secular equilibrium. The ICRP ingestion dose factors are effective dose coefficients calculated as the weighted sum of equivalent doses in all organs and tissues integrated over time (50 y for adults) and consider the biokinetic rates of absorption and excretion of nuclides as well as any progeny produced during their residence time in the human body. It should be noted that the scoping calculations presented here only consider radionuclide ingestion and external dose radiotoxicity is not considered.

4 Time evolution of radionuclide inventory

4.1 Total inventory radiotoxicity

Using the NuDec-Inventory program, the radiotoxicity of the total radionuclide inventory has been calculated as a function of time starting from the 31st of December 2075. This is the reference date used in the compilation of data as supplied (see Section 3.1). The data for radiotoxicity at time of deposition are plotted versus half-life for the reactor waste materials (BHK) in Figure 4-1 and for legacy wastes (BHA) in Figure 4-2. The vertical red line corresponds to a half-life of 10 y, which delineates the cut-off for relevant radionuclides defined in SR-Site (SKB 2010a) and SR-PSU (SKB 2015). Any non-chain fission and activation products to the left of this dividing line can be directly excluded from calculations according to the previously adopted methodology. It can be noted that the inventory of any nuclide with a half-life of 10 y or less will decrease by at least 3 orders of magnitude within the first 100 y post closure. Care must be taken for radionuclides belonging to decay chains, however, since some progeny nuclides (e.g. Po-210, Ra-228) will be produced by ingrowth both in the repository and along migration paths and may contribute towards the far-field dose rate in a non-negligible fashion.

Nuclides with a total radiotoxicity less than 0.1 Sv (horizontal green line) are excluded on the basis that they will contribute negligibly to far-field dose rates relative to the sum of nuclides above this line. It should be noted that many nuclides, which might be considered significant dose contributors at deposition are not present in significant quantities after a few hundred years due to rapid decay (e.g. Sr-90, Cs-137, Co-60). Some progeny nuclides, on the other hand, have significantly increased radiotoxicity owing to ingrowth (e.g. Pb-210, Ac-227).

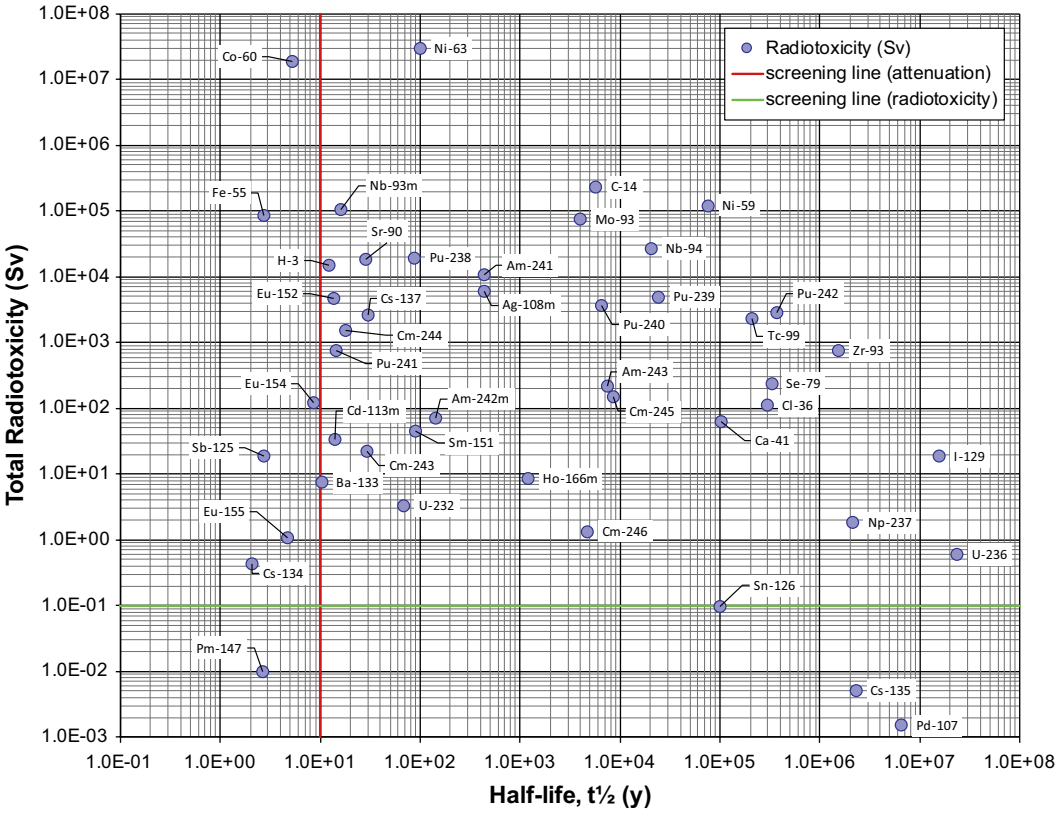

Figure 4-1. *Radiotoxicity at time of deposition plotted as a function of half-life for all nuclides present in the reactor waste (BHK) inventory. The red and green screening lines are the same as those used previously in SR-Site and SR-PSU and are described in the text.*

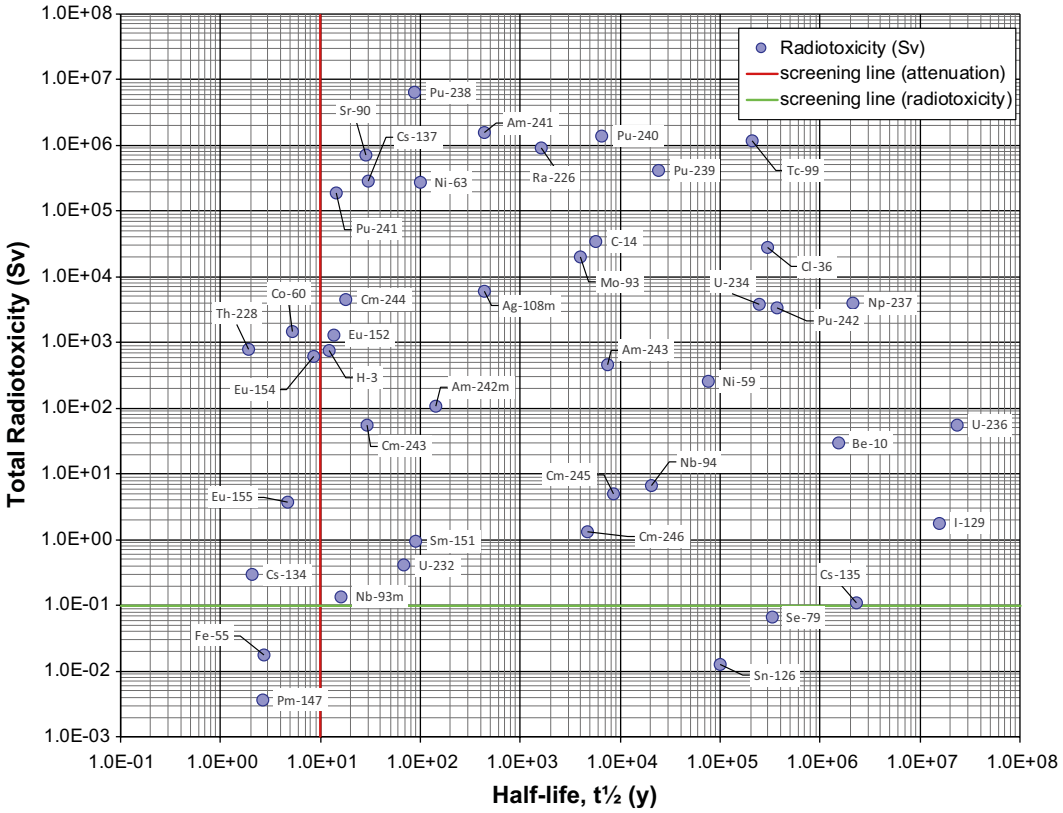

Figure 4-2. *Radiotoxicity at time of deposition plotted as a function of half-life for all nuclides present in the legacy waste inventory (BHA). The red and green screening lines are the same as those used previously in SR-Site and SR-PSU and are described in the text.*

The main systematic differences between the two waste streams are that the legacy waste has a significantly larger inventory of U-234, U-235, U-238, and transuranic elements (with some exceptions for individual progeny nuclides). The reactor wastes, on the other hand, generally contain a much larger inventory of fission and activation products (with the exception of the Cs-134, Cs-135, and Cs-137 isotopes, Cl-36, Tc-99, and Be-10). The legacy wastes are also characterised by much larger proportions of long-lived radionuclides relative to the reactor waste materials.

4.2 Simplification of decay chains

There are 49 radionuclides tabulated in the initial inventory list for the reactor wastes and 53 for the legacy wastes. Taking both waste streams together there are 58 tabulated nuclides. Including the full list of progeny implicit in the decay chains expands the list to a total of 114 radionuclides. Of these, many non-decay chain, or non-actinide (short) chain nuclides can be neglected due to having half-lives less than 10 y in accordance with the decay attenuation selection cut-off discussed previously. Of the remainder, many radionuclide daughters with very short half-lives belonging to actinide decay chains can also be neglected since they can be assumed to be in secular equilibrium with their parent nuclides and are included implicitly in the calculations. In addition to these, Sn-126, Cs-135, and Pd-107 can be discounted due to a total radiotoxicity less than 0.1 Sv. This would give a minimum of about 53 radionuclides necessary to account for the evolution of the inventory over time. The decay chain simplifications for the thorium ($4n$), neptunium ($4n+1$), radium ($4n+2$), and actinium ($4n+3$) series are shown in Figure 4-3 and Figure 4-4. It should be noted that these simplifications have only been used for the NuDec-Farf31 scoping simulations and the time evolution of the inventory using NuDec-Inventory uses the full, unabbreviated decay series.

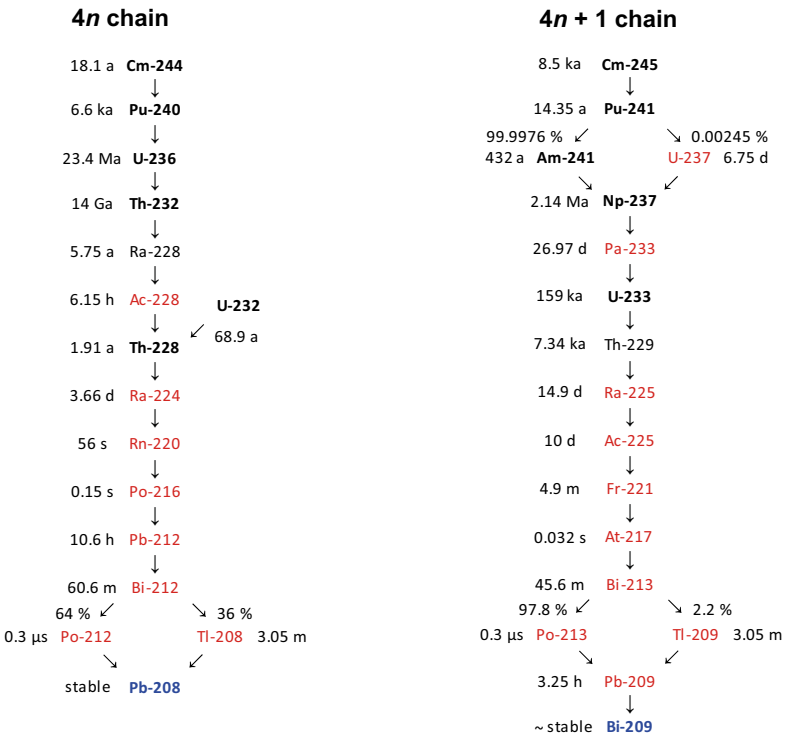

Figure 4-3. *Simplifications to the thorium (4n) and neptunium (4n + 1) series radionuclide decay chains (black bold – explicitly modelled radionuclides included in the initial inventory; black – explicitly modelled radionuclides that are not part of the initial inventory, but where ingrowth occurs; red – radionuclides implicitly modelled assuming secular equilibrium with the parent radionuclide; blue – stable isotope decay chain terminator).*

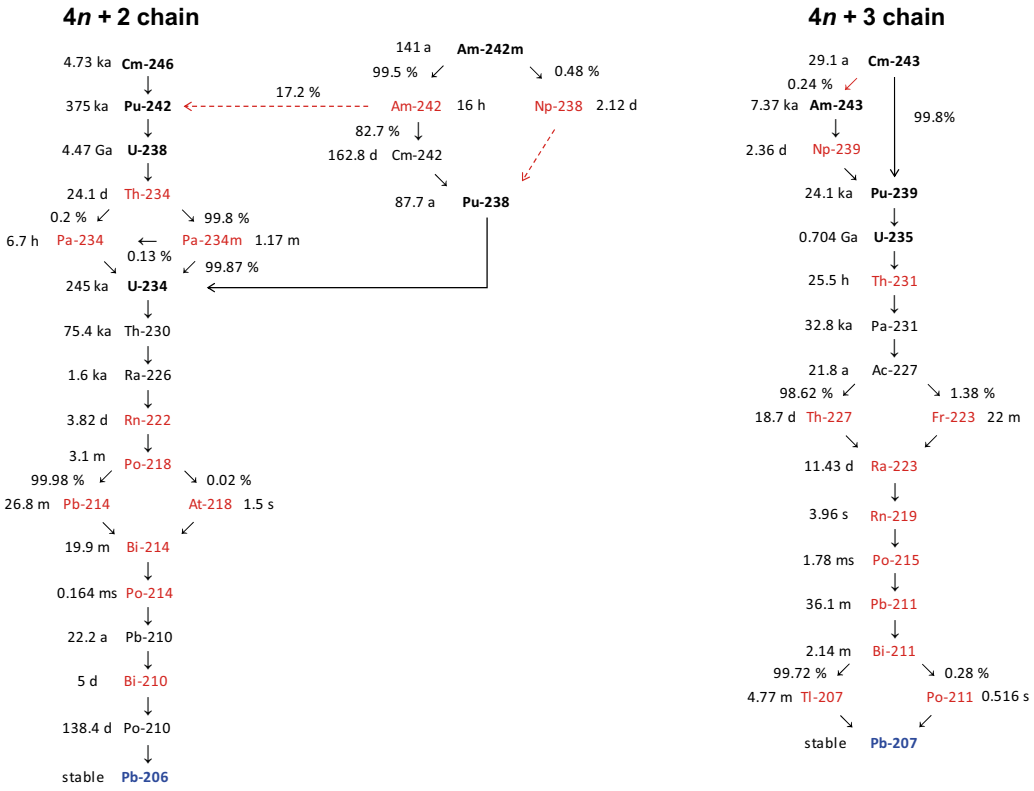

Figure 4-4. *Simplifications to the radium (4n + 2) and actinium (4n + 3) series radionuclide decay chains (black bold – explicitly modelled radionuclides included in the initial inventory; black – explicitly modelled radionuclides that are not part of the initial inventory, but where ingrowth occurs; red – radionuclides implicitly modelled assuming secular equilibrium with the parent radionuclide; blue – stable isotope decay chain terminator). Red arrows indicate neglected pathways for far-field scoping calculations using Farf31.*

Although it is possible to considerably shorten the list of radionuclides as outlined above, the NuDec-Inventory program is sufficiently fast that no simplification is necessary, and the evolution of the full inventory can be easily simulated for arbitrarily long timescales. There is also no restriction on the calculation of converging or diverging radionuclide chains with the program, which is not always the case for far-field transport codes.

The current release version of the stand-alone Farf31 code, on the other hand, is limited to a maximum of 48 radionuclides consisting of no more than 32 distinct elements and no chain is permitted to have more than 8 members. Additionally, it cannot simulate converging or diverging decay processes. In the present case, diverging chains are mostly trivial and can be neglected due to short half-lives and the fact that they are implicitly modelled in the abbreviated decay chain models. The converging chains, however, cannot be neglected since they can contribute in a non-negligible fashion to the ingrowth of nuclide progeny and therefore need to be properly accounted for.

For the reactor and legacy wastes there are 58 tabulated radionuclides representing 40 distinct elements and 4 additional converging chains that need to be considered in far-field transport calculations. This includes the 3 separate converging chains shown in Figure 4-3 and Figure 4-4 as well as the decay process involving Mo-93 and Zr-93 with the common Nb-93m daughter nuclide. Removing the trivially short-lived or very low inventory nuclides gives a total of 53 as indicated in Table 4-1. Fortunately, many of the Farf31 code restrictions outlined above can be circumvented by smart pre- and post-processing with the aid of the NuDec-Farf31 interface. This is achieved by splitting the problem up into a number of sub-problems and then recombining and summing the results in post-processing. In order to do this each of the non-chain, short chain, and actinide chain subsets are simulated separately as well as additional converging subsets where relevant. This gives a total of 10 separate simulations necessary to account for the far-field transport using Farf31. For the converging chains where the same progeny appear in multiple simulations, care is taken to ensure that the initial source term for the daughter nuclide is included only once (i.e. ingrowth is only considered for the subsequent converging chains).

The NuDec-Farf31 interface takes care of the simulation subsets automatically and concatenates the results without any additional input from the user apart from the abbreviated chain definitions given in Table 4-1 and hydrodynamic transport parameters (F-factor and advective travel time) for geosphere migration calculations. Material properties for the geosphere are automatically loaded from a user selected, task-specific database (discussed in more detail in Appendix A). In the present case, the same material properties are assumed as defined for the Laxemar site in the SR-Site project (SKB 2010c, Appendix A) with some additions taken from Crawford (2013) as were documented in an early draft version of the SE-SFL radionuclide transport data set. It is noted that the nuclides listed as short-chain are effectively non-chain nuclides due to the fast decay of daughter nuclides and only the Mo-93, Zr-93, Nb-93m system needs to be modelled explicitly. An example of a result for a converging chain is shown in Figure 4-5 for the decay of Mo-93 and Zr-93 with the common daughter nuclide Nb-93m. The example calculation is based on the initial BHK inventory assuming a simple near-field release boundary condition in proportion to the total inventory and neglecting source depletion.

Table 4-1. Minimum abbreviated set of 53 radionuclides necessary to simulate evolution of radionuclide inventory and far-field transport in the geosphere using the NuDec-Farf31 program. Separate converging chains are given as Subset 1 and Subset 2. Progeny in Subset 2 that are common to both converging chains are coloured red and their source term only needs to be considered once (ingrowth only in the subordinate chain). Very short lived non-ingrowing radionuclides ($t_{½}$ ≤ 10 y) and those with insignificant inventories (≤ 0.1 Sv total radiotoxicity) are not included.

Chain ID	Subset 1	Subset 2
4*n*	Cm-244	
	Pu-240	
	U-236	
	Th-232	
	Ra-228	U-232
	Th-228	Th-228
4*n* + 1	Cm-245	
	Pu-241	
	Am-241	
	Np-237	
	U-233	
	Th-229	
4*n* + 2	Cm-246	Am-242m
	Pu-242	Cm-242
	U-238	Pu-238
	U-234	U-234
	Th-230	Th-230
	Ra-226	Ra-226
	Pb-210	Pb-210
	Po-210	Po-210
4*n* + 3	Cm-243	Am-243
	Pu-239	Pu-239
	U-235	U-235
	Pa-231	Pa-231
	Ac-227	Ac-227
Non-chain	Ag-108m	
	Ba-133	
	Be-10	
	C-14	
	Ca-41	
	Cd-113m	
	Cl-36	
	H-3	
	Ho-166m	
	I-129	
	K-40	
	Nb-94	
	Ni-59	
	Ni-63	
	Se-79	
	Sm-151	
Short-chain	Cs-137	
	Eu-152	
	Mo-93	Zr-93
	Nb-93m	Nb-93m
	Sr-90	
	Tc-99	

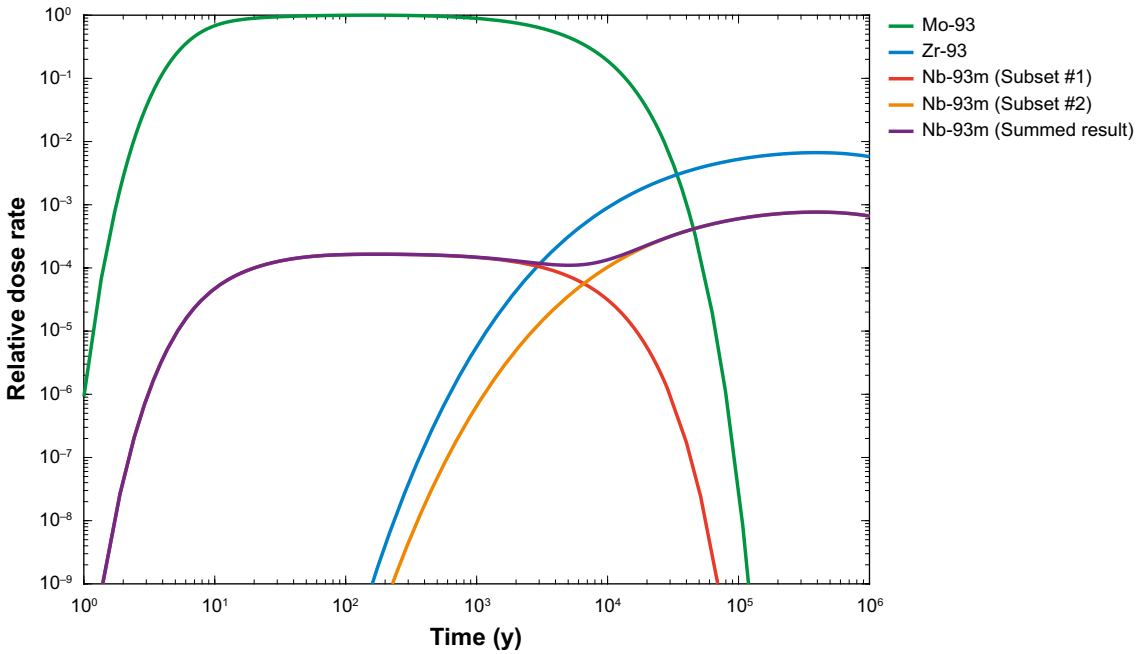

Figure 4-5. *Example showing how results from 2 separate Farf31 migration simulations are combined to give the overall summed breakthrough for a converging chain with a common daughter nuclide. Results are shown for two separate simulations considering Mo-93 decay to Nb-93m and Zr-93 to Nb-93m and the combined breakthrough of Nb-93m obtained by summing the results for ingrowth of Nb-93m in both simulation subsets. The relative dose rate contributed by each sub-chain is plotted in the figure relative to Mo-93 (radiotoxicity flux (Sv/y) normalised by the peak radiotoxicity flux (Sv/y) of Mo-93).*

4.3 Reactor waste inventory (BHK)

Figure 4-6 shows the evolution of inventory radiotoxicity over time for reactor waste nuclides. Only those nuclides whose peak radiotoxicities in the time interval 1 y–100 ky account for more than a 10^{-6} fraction of the total radiotoxicity (broken curve) are shown. It should be noted that the total specified in the figure legend is the maximum value of the summed individual radiotoxicities as shown in the figure and not the sum of individual peak values given in the legend since peak contributions occur at different times. Figure 4-7 shows the evolution where the screening time interval is taken instead to be the period from 0.1 ky–100 ky. In both figures, the values given in the legend indicate the maximum equivalent radiotoxicity of each ranked nuclide during the screening time period. As can be seen from Figure 4-7, a number of the fast decaying radionuclides (Co-60, Fe-55, Sr-90, H-3, Eu-152, Cm-244, Pu-241, Eu-154) are found to make a negligible contribution to radiotoxicity already 100 y after closure. Although decaying rapidly, the Cm-244 and Pu-241 radionuclides cannot be neglected, however, since they are necessary to establish the correct inventory of daughter nuclides in the $4n$ and $4n+1$ decay chains. It can also be noted that the Ni-59 and Ni-63 radioisotopes together with C-14, Mo-93, and Nb-94 account for the bulk of the reactor waste radiotoxicity in the screening time interval of 0.1–100 ky. There are not large amounts of long-lived radionuclides in the reactor wastes which is why the total radiotoxicity decreases by about 3 orders of magnitude in the first 100 ky.

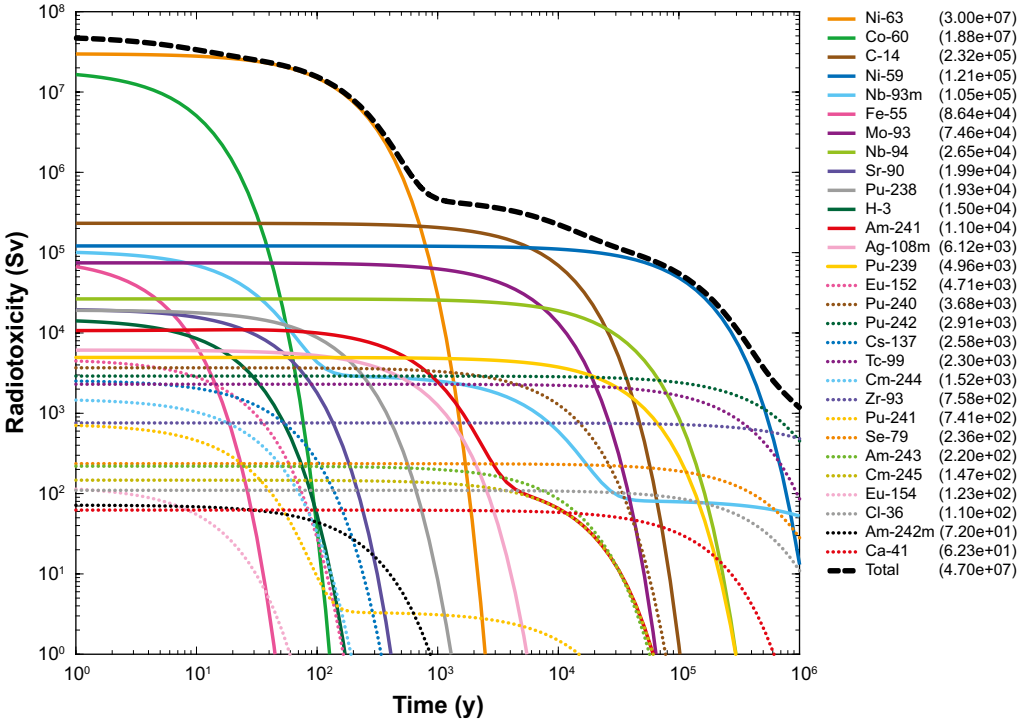

Figure 4-6. *Evolution of reactor waste (BHK) inventory radiotoxicity as a function of time. Radionuclides are listed in the legend in order of peak radiotoxicity contribution in the time interval 1 y–100 ky (units in Sv). Only radionuclides whose peak radiotoxicity contributes more than an equivalent fraction of 10^{-6} of the total radiotoxicity at any given time are plotted.*

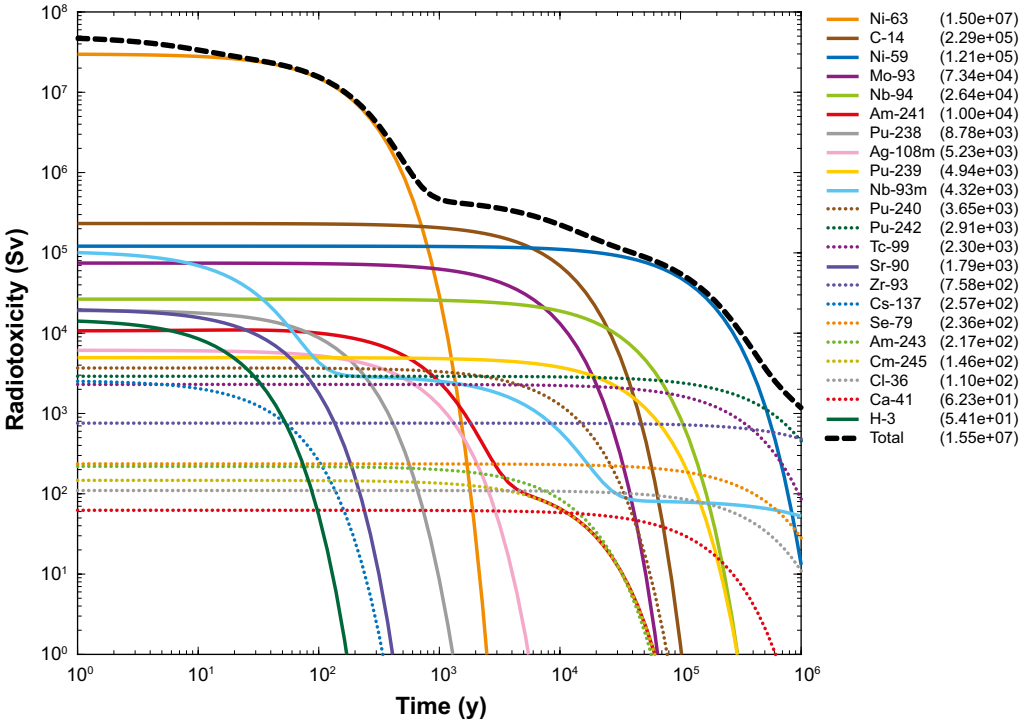

Figure 4-7. *Evolution of reactor waste (BHK) inventory radiotoxicity as a function of time. Radionuclides are listed in the legend in order of peak radiotoxicity contribution in the time interval 0.1 ky–100 ky (units in Sv). Only radionuclides whose peak radiotoxicity contributes more than an equivalent fraction of 10^{-6} of the total radiotoxicity at any given time are plotted.*

4.4 Legacy waste inventory (BHA)

Figure 4-8 shows the evolution of inventory radiotoxicity over time for legacy waste nuclides. As previously, only those nuclides whose peak radiotoxicities in the time interval 1 y–100 ky account for more than a 10^{-6} fraction of the total radiotoxicity (broken curve) are shown. As previously, the total specified in the figure legend is the maximum value of the summed individual radiotoxicities as shown in the figure and not the sum of individual peak values given in the legend since peak contributions occur at different times. Figure 4-9 shows the evolution where the screening time interval is taken instead to be the period from 0.1 ky–100 ky. In both figures, the values given in the legend indicate the maximum equivalent radiotoxicity of each ranked nuclide during the screening time period. As can be seen from Figure 4-9, a number of the fast decaying radionuclides (Co-60, Ru-106, Fe-55, H-3, Eu-155, Eu-154, Eu-152, Cm-243) are found to make a negligible contribution to radiotoxicity already 100 y after closure as the screening calculation shows. The Cm-243 radionuclide cannot be neglected, however, since it is necessary to establish the correct inventory of daughter nuclides in the $4n+3$ decay chain. It can be noted that the daughter nuclides from the actinide decay chains (the radium chain, $4n+2$ in particular) and Tc-99 account for bulk of the legacy waste radiotoxicity in the screening time interval of 0.1 ky–100 ky. The larger proportion of long-lived radionuclides in the legacy waste can be clearly appreciated from the total radiotoxicity, which decreases by only about an order of magnitude over the first 100 ky although this behaviour is mostly attributable to the very large inventory of Tc-99.

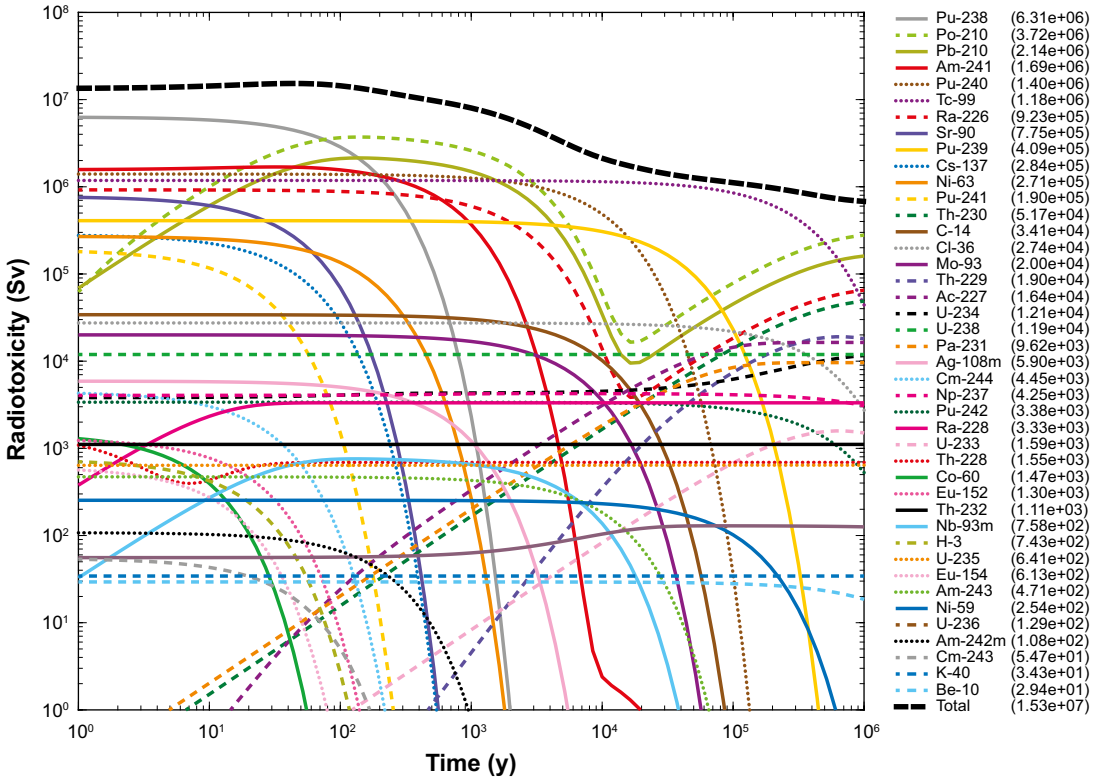

Figure 4-8. *Evolution of legacy waste (BHA) inventory radiotoxicity as a function of time. Radionuclides are listed in the legend in order of peak radiotoxicity contribution in the time interval 1 y–100 ky (units in Sv). Only radionuclides whose peak radiotoxicity contributes more than an equivalent fraction of 10^{-6} of the total radiotoxicity at any given time are plotted.*

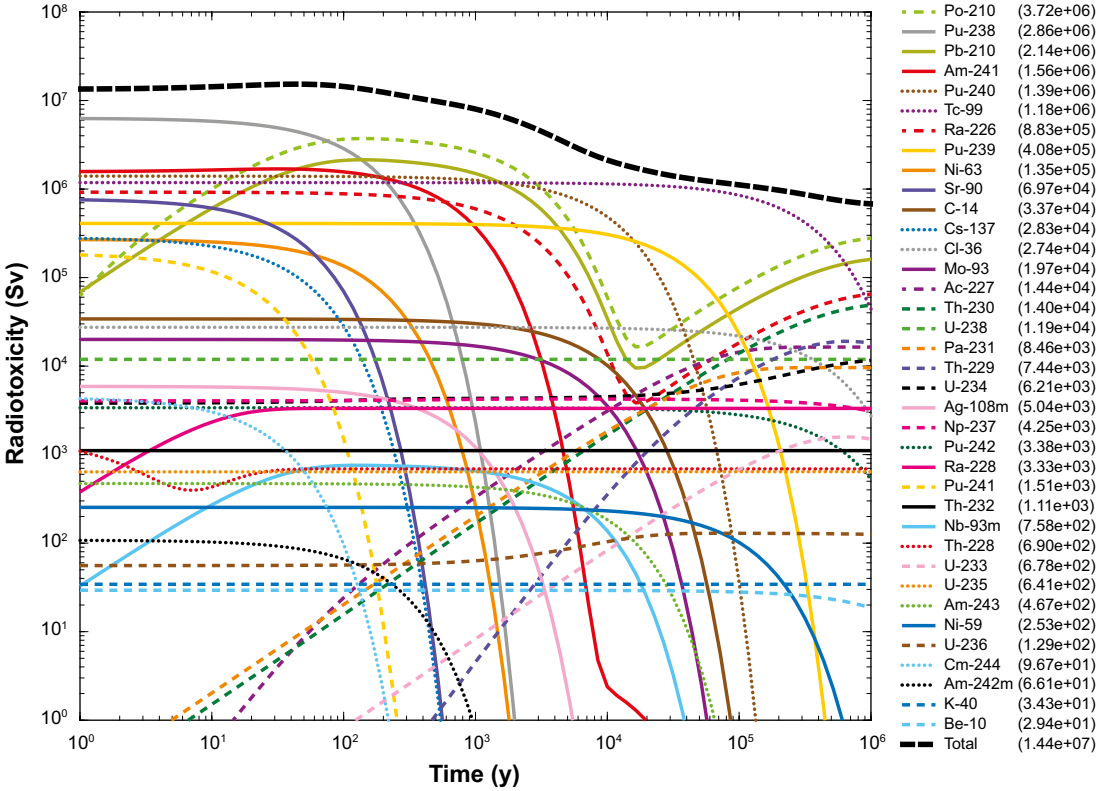

Figure 4-9. *Evolution of legacy waste (BHA) inventory radiotoxicity as a function of time. Radionuclides are listed in the legend in order of peak radiotoxicity contribution in the time interval 0.1 ky–100 ky (units in Sv). Only radionuclides whose peak radiotoxicity contributes more than an equivalent fraction of 10^{-6} of the total radiotoxicity at any given time are plotted.*

4.5 Radionuclide inventory derived from ESS (European Spallation Source) operations

Since the plans for the construction and operation of the European Spallation Source, ESS, are not yet finalised, only limited information is available concerning amount and composition of the waste from ESS. The data presented here are taken from Table 5.1 in a technical report[3], which was made available to the author in the form of a pdf document. It is noted that the base year for the calculations is 2060 rather than 2075 as assumed for the reactor and legacy waste inventories (see Section 3.1).

Some of the half-lives included in the technical report from ESS differ from those used previously in SR-PSU and those given by Firestone et al. (1999) for novel nuclides not previously considered in SKB safety assessments. Taking into consideration that half-lives were variously rounded to one or two significant figures in the data compilation, the present author has only considered deviations greater than 10 % as being significant. For the nuclides that exhibit only minor deviations (i.e. < 10 %), however, the rounding of significant figures appears to be consistent with the error estimate of the underlying half-life estimates in Firestone et al. (1999) and is not of major concern. The deviations (> 10 %) are listed in Table 4-2.

From Table 4-2 it appears that the half-lives for Se-79, Nb-91, and Tb-157 in the compilation in the technical report from ESS are typographical errors, whereas deviations for the remaining nuclides seem to be due to genuine differences in the underlying data and those complied by Firestone et al. (1999). Although many of the nuclides present in the ESS compilation are activation products of metals and rare earth elements used in alloys, there are a number of fission products that are also present in the reactor and legacy waste materials. The radiotoxicity of the waste in the compilation in the technical

[3] Persson P, 2018. Characteristics of radioactive waste from ESS to be disposed in SKB facilities. Technical Report, Document number ESS-0036701, Revision 2(3), SKBdoc 1701742 ver 1.0, Svensk Kärnbränslehantering AB.

report from ESS for the base year 2060 is plotted in Figure 4-10. The radiotoxicity for Ar-39 is not plotted since it is an inert gas and may therefore be excluded from ingestion based far-field radiotoxicity calculations. It should be noted that a small number of nuclides in the ESS compilation appear to not have ICRP-quantified dose conversion factors and therefore their radiotoxicity is largely unknown (and thus cannot be plotted in Figure 4-10). These nuclides are tabulated in Table 4-3.

Table 4-2. Differences between radionuclide half-lives used in the technical report from ESS and those used in this work (based on values previously in SKB safety assessments and the compilation by Firestone et al. (1999) for novel nuclides not previously considered in SKB safety assessments). Due to rounding to between one and two significant figures in the data provided in the technical report from ESS, only nuclides whose half-lives differ by more than 10 % are shown.

Nuclide	Technical report ESS	This work	Difference %
Si-32	130 y	150 y	13.3
Ti-44	47 y	63 y	25.4
Se-79	3.3×10^4 y	3.27×10^5 y	89.9
Kr-81	2.0×10^5 y	2.29×10^5 y	12.7
Nb-91	68 y	680 y	90
Mo-93	3.5×10^3 y	4.0×10^3 y	12.5
Tc-97	3.0×10^6 y	2.6×10^6 y	−15.4
Tb-157	150 y	71 y	−111.3
Tb-158	150 y	180 y	16.7

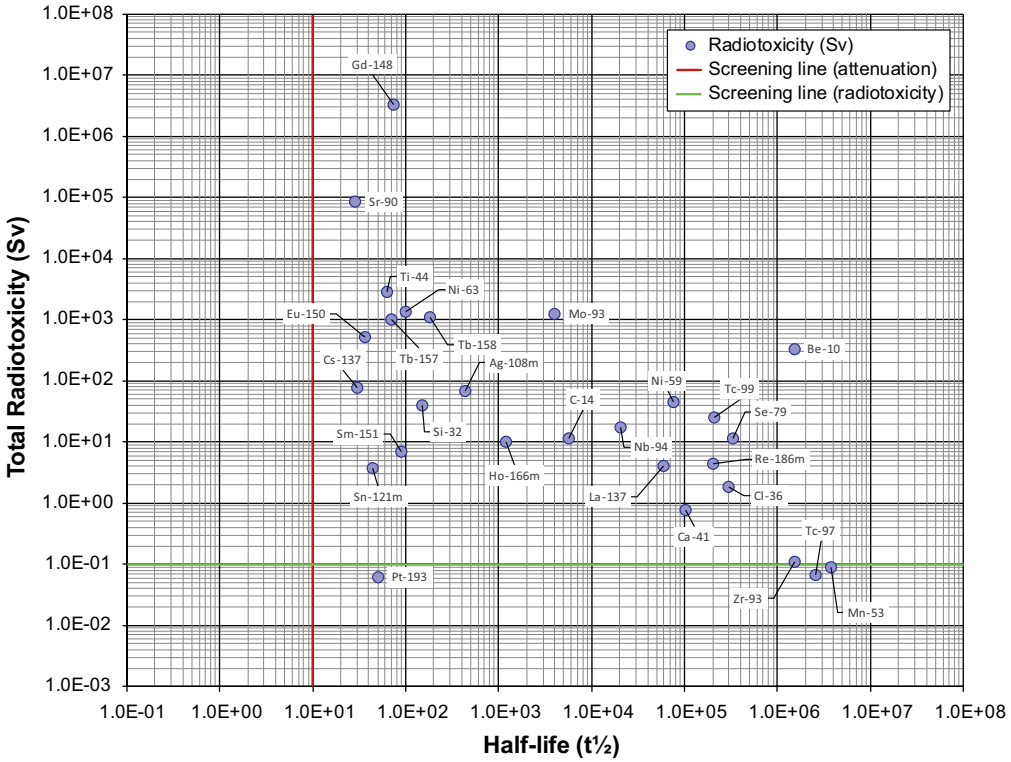

Figure 4-10. *Radiotoxicity at the reference year 2060 plotted as a function of half-life for all nuclides present in the compilation in the technical report from ESS that have quantified dose conversion factors. Nuclides that have unknown dose conversion factors not documented in the ICRP tables (i.e. neither ICRP 1995 nor ICRP 2012) are not shown, although are discussed in the text. The red and green screening lines are the same as those used previously in SR-Site and SR-PSU and are described in the text.*

Table 4-3. Nuclides in the ESS waste inventory for which no dose conversion factors are available in the ICRP tables (i.e. neither ICRP 1995 nor ICRP 2012). Decay modes are: β^- (beta), EC (electron capture), β^+ (positron), α (alpha), γ (gamma), IT (isomeric transition).

Nuclide	Half-life	Decay mode	Activity (Bq)
Ar-42	32.9 y	β^- (600 keV)	4.0×10^{11}
Nb-91	680 y	EC/β^+ (n/a)	2.0×10^{12}
Gd-150	1.79×10^6 y	α (~2.73 MeV)	2.0×10^9
Dy-154	3.0×10^6 y	α (~2.87 MeV)	1.0×10^9
Ho-163	4.57×10^3 y	EC	2.0×10^{12}
Hf-178m2	31 y	IT/γ (n/a)	1.0×10^{12}

All of the radionuclides in the ESS inventory are either single nuclides that decay to stable elemental states, or short (non-actinide) chain nuclides with one, or at most two daughter nuclides. Most of the progeny from the short chain nuclides have very short half-lives and thus would be in secular equilibrium and therefore included in the dose factor for the parent. Three exceptions are Sm-151, Dy-154, and Gd-150 which have progeny with exceptionally long half-lives. The daughter product of Sm-151 decay, in particular, (Eu-151) has a half-life of 4.62×10^{18} y and can be considered to be effectively stable. Dy-154, on the other hand, decays to Gd-150 (half-life 1.79×10^6 y), while Gd-150 decays to Sm-146 (half-life 1.03×10^8 y). The decay of Gd-150 gives rise to a slow ingrowth of Sm-146, although this daughter can be mostly neglected for times less than 1 Ma.

Of the nuclides depicted in Figure 4-10, four have radiotoxic inventories that are intermediate between those residing in the reactor and legacy waste streams, 10 have radiotoxic inventories much less than the other waste streams, while 13 are unique to the ESS waste and therefore represent maximum radiotoxicities for those nuclides. The nuclides with "intermediate" radiotoxic inventories are tabulated Table 4-4, while nuclides belonging to the "maximum" radiotoxic inventory group are tabulated in Table 4-5. The remaining nuclides with low radiotoxic inventories relative to the reactor and legacy wastes are tabulated in Table 4-6.

Table 4-4. Nuclides in the ESS waste which have radiotoxicity inventories residing in between the corresponding nuclide radiotoxicity in the reactor and legacy waste streams.

nuclide	Half-life	ESS (Sv)	BHK (Sv)	BHA (Sv)
Se-79	3.27×10^5 y	11.6	236	0.0662
Sr-90	28.8 y	8.40×10^4	1.79×10^4	7.06×10^5
Nb-94	2.03×10^4 y	17.0	2.65×10^4	6.57
Sm-151	90 y	6.86	44.2	0.961

Table 4-5. Nuclides in the ESS waste which are either unique to that waste stream or have radiotoxicities much greater than the corresponding inventory in the BHK or BHA waste streams (affects Be-10 only).

Nuclide	Half-life	ESS (Sv)	BHK (Sv)	BHA (Sv)
Be-10	1.51×10^6 y	330	7.05×10^{-5}	29.4
Si-32	150 y	39.2	n/a	n/a
Ar-39	269 y	~0 (4.4 Sv, inhalation)	n/a	n/a
Ti-44	63.0 y	2.9×10^3	n/a	n/a
Mn-53	3.74×10^6 y	0.09	n/a	n/a
Kr-81	2.29×10^5 y	~0 (0.063 Sv, inhalation)	n/a	n/a
Tc-97	2.60×10^6 y	0.068	n/a	n/a
La-137	6.0×10^4 y	4.05	n/a	n/a
Eu-150	36.9 y	520	n/a	n/a
Gd-148	74.6 y	3.36×10^6	n/a	n/a
Tb-157	71.0 y	1.02×10^3	n/a	n/a
Tb-158	180 y	1.10×10^3	n/a	n/a
Re-186m	2.0×10^5 y	4.4	n/a	n/a
Pt-193	50 y	0.062	n/a	n/a

Table 4-6. Nuclides in the ESS waste which have significantly lower inventories than either the reactor or legacy waste streams (some nuclides are not present in both reactor and legacy waste streams).

Nuclide	Half-life	ESS (Sv)	Reactor (Sv)	Legacy (Sv)
C-14	5.73×10^3 y	11.6	2.31×10^5	3.41×10^4
Cl-36	3.01×10^5 y	1.86	110	2.74×10^4
Ca-41	1.03×10^5 y	0.76	62.3	n/a
Ni-59	7.6×10^4 y	44.1	1.21×10^5	254
Ni-63	100	1.35×10^3	2.99×10^7	2.71×10^5
Zr-93	1.53×10^6 y	0.11	758	n/a
Mo-93	4.0×10^3 y	1.24×10^3	7.39×10^4	2.0×10^4
Tc-99	2.11×10^5 y	25.6	2.27×10^3	1.18×10^6
Ag-108m	438 y	69.1	6.30×10^3	5.9×10^3
Cs-137	30.2 y	78.0	2.44×10^3	2.84×10^5

As previously mentioned, the plans for the construction and operation of ESS are not yet finalised, and only limited information is available concerning amount and composition of the waste from ESS. Due to the aforementioned uncertainties, the waste volume and amount of material from ESS are not taken into account in the safety evaluation of SFL. Instead, only radionuclides that are unique to that waste stream (Table 4-5) are included. Further, the nuclides Mn-53, Tc-97, and Pt-193 are excluded from dose calculations on account of having an inventory lower than the screening level of 0.1 Sv as discussed in previous sections. The inert gases Ar-39 and Kr-81 can be excluded from geosphere transport calculations on account of low solubility in mobile groundwater, although Ar-39 might need to be considered in gas phase transport screening calculations. The resulting list of ESS-specific radionuclides is given in Table 4-7.

Table 4-7. ESS-specific radionuclides included in the SFL safety evaluation.

Nuclide	Half-life
Si-32	150 y
Ar-39	269 y
Ti-44	63.0 y
La-137	6.0×10^4 y
Eu-150	36.9 y
Gd-148	74.6 y
Tb-157	71.0 y
Tb-158	180 y
Re-186m	2.0×10^5 y

5 Ranking of dose dominant radionuclides in geosphere transport

In this section, the transport of radionuclides described in Section 4.3 and 4.4 is simulated using Farf31 (using the NuDec-Farf31 interface as described previously). Reference calculations have been made for an F-factor of 5.37×10^4 y/m and an advective travel time of 6.4 y corresponding to the central corrosion case in SR-Site (SKB 2010a)[4]. Additional screening calculations have also been made for an advective travel time of 10 y and F-factors in the range 10^3–10^6 y/m. An F-factor of 10^3 y/m represents a flowpath with poor retardation potential, whereas an F-factor of 10^6 y/m might be regarded as exhibiting good retardation potential. In all screening cases, a Péclet number of 10 has been assumed for the hydrodynamic dispersivity. Material properties for geosphere transport were largely based on the values used in SKB (2010c), although with some values taken from Crawford (2013). The K_d values used in these calculations are given in Table 5-1. All K_d data used here were taken directly from an early draft version of the data set to be used in SE-SFL and may not necessarily correspond to the values used in the final geosphere transport modelling. The results of the transport calculations presented in this report should therefore be considered as purely indicative.

Two separate, near-field transport source terms (radionuclide flux boundary conditions) for the BHK and BHA vaults were preliminarily provided by SKB and have been used in our geosphere transport screening calculations (65 radionuclides consisting of 41 distinct radioelements). These preliminary data were provided in the form of Microsoft Excel files. The source term delivery provides no information on uncertainty or spatial variability, apart from the fact that each vault is assigned its own source term. The source term is specified for logarithmically spaced time steps up until 10 million years after repository closure, although the calculations presented in this report only consider the first one million years. In the delivery, the BHK source term includes ESS radionuclides, but one of the tasks of SE-SFL is to evaluate which vault, i.e. BHA or BHK, is the most favourable for storage of the ESS waste. Hence, this delivery can be seen as coming from a "what if" case, as delivered from the near-field modelling, investigating the radionuclide releases of ESS nuclides should this waste type be stored in the BHK vault. The calculations presented in this section constitute a simulation of transport retardation for a range of different hydrodynamic conditions and consider geosphere migration processes only. The breakthrough curves shown for "far-field" transport in each case study therefore represents the flux of radionuclides exiting the geosphere and entering the biosphere.

[4] Note that the advective travel time of 6.4 y was rounded to 6 y in the Table 4-2 and Table 4-3 of the reference (SKB 2010a)

Table 5-1. K_d values used in the geosphere transport scoping calculations discussed in this report. References and comments are given for the sources of values used.

Radioelement	K_d (m^3/kg)	Reference	Comment
Ac	1.48×10^{-2}	SKB 2010c, Table A8-4	Best estimate value
Ag	6.54×10^{-4}	SKB 2010c, Table A8-4	Best estimate value
Am	1.48×10^{-2}	SKB 2010c, Table A8-4	Best estimate value
Ar	0		Conservative assumption
Ba	1.0×10^{-3}	Crawford 2013, Table 6-1	Best estimate, T-Sal groundwater
Be	0		Conservative assumption
Ca	0	Crawford 2013, Table 6-1	Best estimate
Cd	2.07×10^{-3}	SKB 2010c, Table A8-4	Best estimate
C-inorg	0	SKB 2010c, Table A8-4	Best estimate, HCO_3^-
C-org	0	SKB 2010c, Table A8-4	Best estimate, CH4, -CO_2H
Cl	0	SKB 2010c, Table A8-4	Best estimate value
Cm	1.48×10^{-2}	SKB 2010c, Table A8-4	Best estimate value
Co	7.40×10^{-4}	Crawford 2013, Table 6-1	Best estimate value
Cs	6.54×10^{-4}	SKB 2010c, Table A8-4	Best estimate value
Eu	1.48×10^{-2}	SKB 2010c, Table A8-4	Best estimate value
Gd	0		Conservative assumption
H	0	SKB 2010c, Table A8-4	Best estimate value
Ho	1.48×10^{-2}	SKB 2010c, Table A8-4	Best estimate value
I	0	SKB 2010c, Table A8-4	Best estimate value
K	0		Conservative assumption
La	0		Conservative assumption
Mo	0	SKB 2010c, Table A8-4	Best estimate value
Nb	1.98×10^{-2}	SKB 2010c, Table A8-4	Best estimate value
Ni	2.07×10^{-3}	SKB 2010c, Table A8-4	Best estimate value
Np	9.92×10^{-2}	SKB 2010c, Table A8-4	Best estimate value, Np(IV)
Pa	5.92×10^{-2}	SKB 2010c, Table A8-4	Best estimate value, Pa(V)
Pb	2.52×10^{-2}	SKB 2010c, Table A8-4	Best estimate value
Pd	5.2×10^{-2}	SKB 2010c, Table A8-4	Best estimate value
Po	0	Crawford 2013, Table 6-2	Best estimate value, Po(-II, II, VI)
Pu	2.78×10^{-2}	SKB 2010c, Table A8-4	Best estimate value, Pu(III)
Ra	4.53×10^{-4}	SKB 2010c, Table A8-4	Best estimate value
Re	0		Conservative assumption
Se	2.95×10^{-4}	SKB 2010c, Table A8-4	Best estimate value, Se(-II)
Si	0		Conservative assumption
Sm	1.48×10^{-2}	SKB 2010c, Table A8-4	Best estimate value
Sr	6.42×10^{-6}	SKB 2010c, Table A8-4	Best estimate value
Tb	0		Conservative assumption
Tc	9.92×10^{-2}	SKB 2010c, Table A8-4	Best estimate value, Tc(IV)
Th	5.29×10^{-2}	SKB 2010c, Table A8-4	Best estimate value
Ti	0		Conservative assumption
U	2.00×10^{-4}	SKB 2010c, Table A8-4	Best estimate value, U(VI)
Zr	2.13×10^{-2}	SKB 2010c, Table A8-4	Best estimate value

5.1 Dose dominant radionuclides derived from the reactor waste (BHK) inventory

The preliminary near-field source term for the reactor waste (BHK) inventory is shown in Figure 5-1, although converted from units of Bq/y to the equivalent radiotoxicity flux, µSv/y. The delivered preliminary near-field source term for BHK in Bq/year is shown in Appendix B.

The breakthrough of various radionuclides is shown in Figure 5-2 for the reference case hydrodynamic parameters ($F = 5.37 \times 10^4$ y/m, $t_w = 6.4$ y) and the source term shown in Figure 5-1.

Table 5-2 shows the results of the NuDec-Farf31 migration screening calculations for the reactor waste and various F-factors representing a broad range of hydrodynamic transport resistances likely to be encountered in the geosphere. The top 10 potentially dose contributing nuclides are ordered in terms of their far-field peak dose contribution at any time in the period 0.1 ky–100 ky. The associated numerical values are peak values of equivalent transported radiotoxicity expressed as a fraction of the total peak source radiotoxicity. It should be noted that these screening calculations are only intended to give a rough indication of which radionuclides might reasonably be expected to be of most importance in more detailed transport calculations and are highly dependent on the underlying assumptions of the source term.

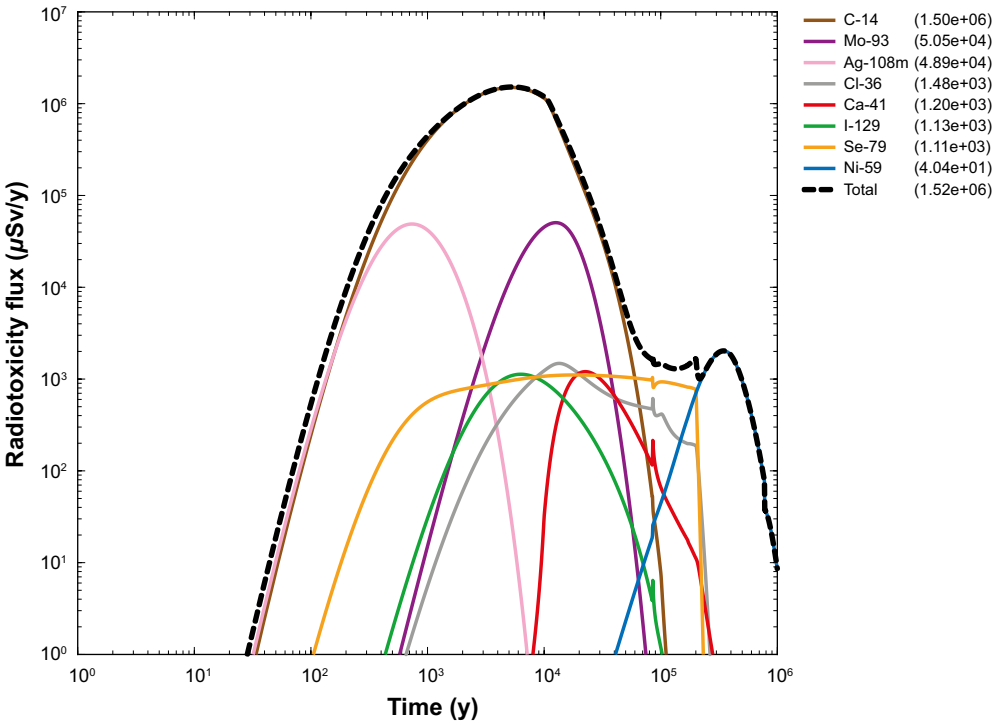

Figure 5-1. *Near-field source term for reactor waste (BHK) radiotoxicity as a function of time from release start. This is based on an early preliminary delivery. Radionuclides are listed in the legend in order of peak contribution to total radiotoxicity in the interval 0.1 ky–100 ky (units in µSv/y). Only radionuclides whose peak radiotoxicity contributes more than an equivalent fraction of 10^{-6} of the total peak source radiotoxicity are plotted.*

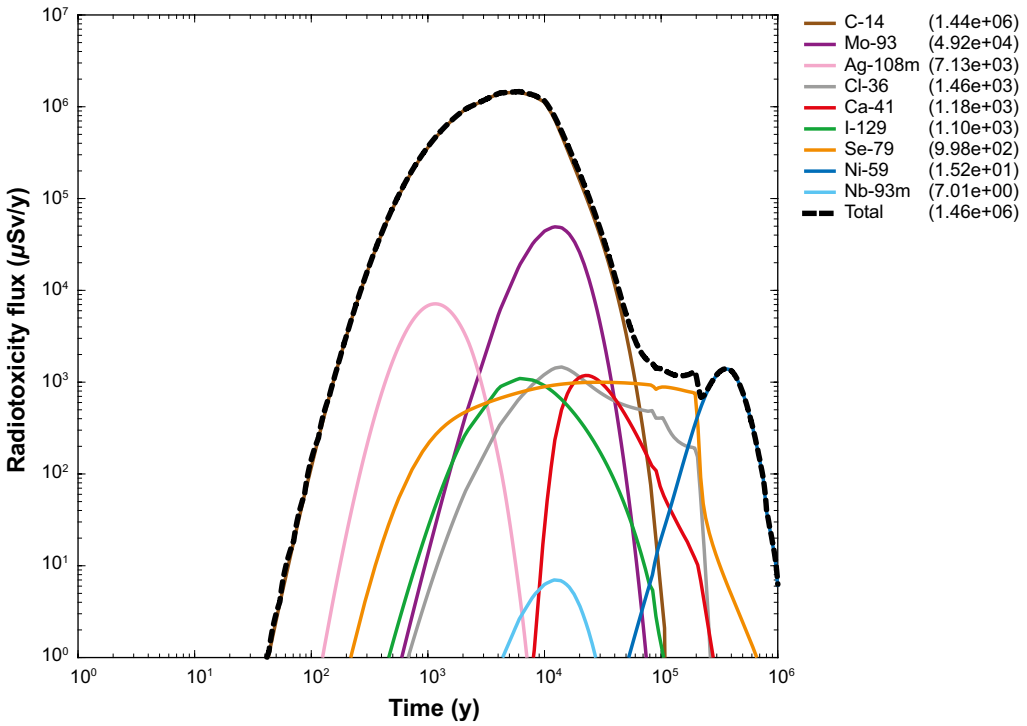

Figure 5-2. *Far-field breakthrough curves for transported reactor waste (BHK) radiotoxicity as a function of time (t_w = 6.4 y, F = 5.4×10⁴ y/m). Radionuclides are listed in the legend in order of peak contribution to total radiotoxicity in the interval 0.1 ky–100 ky (units in µSv/y). Only radionuclides whose peak radiotoxicity contributes more than an equivalent fraction of 10^{-6} of the total peak radiotoxicity are plotted.*

Table 5-2. Results of screening calculations indicating top 10 potentially dose contributing nuclides for reactor wastes and various F-factors for the time interval 0.1–100 ky. Values indicate the peak transported radiotoxicity expressed as a fraction of the total peak source radiotoxicity.

t_w	10 y		10 y		10 y		10 y
F-factor	10^3 y/m		10^4 y/m		10^5 y/m		10^6 y/m
C-14	9.75×10^{-1}	C-14	9.70×10^{-1}	C-14	9.23×10^{-1}	C-14	5.77×10^{-1}
Mo-93	3.29×10^{-2}	Mo-93	3.29×10^{-2}	Mo-93	3.19×10^{-2}	Mo-93	2.39×10^{-2}
Ag-108m	3.303×10^{-2}	Ag-108m	2.10×10^{-2}	Ag-108m	1.31×10^{-3}	Cl-36	8.14×10^{-4}
Cl-36	9.72×10^{-4}	Cl-36	9.69×10^{-4}	Cl-36	9.55×10^{-4}	Ca-41	6.02×10^{-4}
Ca-41	7.89×10^{-4}	Ca-41	7.89×10^{-4}	Ca-41	7.67×10^{-4}	I-129	4.96×10^{-4}
I-129	7.41×10^{-4}	I-129	7.36×10^{-4}	I-129	7.05×10^{-4}	Se-79	2.01×10^{-4}
Se-79	7.28×10^{-4}	Se-79	7.15×10^{-4}	Se-79	6.08×10^{-4}	Nb-93m	3.16×10^{-7}
Nb-93m	2.38×10^{-4}	Nb-93m	3.79×10^{-4}	Ni-59	5.65×10^{-6}	Ag-108m	5.93×10^{-9}
Ni-59	2.57×10^{-5}	Ni-59	2.21×10^{-5}	Nb-93m	3.81×10^{-6}	Ni-59	1.73×10^{-9}
H-3	3.10×10^{-7}	H-3	2.86×10^{-7}	H-3	1.36×10^{-7}	Cs-135	1.73×10^{-9}

5.2 Dose dominant radionuclides derived from the legacy waste (BHA) inventory

The preliminary source term for the legacy waste (BHA) inventory as delivered is shown in Figure 5-3, although converted from units of Bq/y to the equivalent radiotoxicity flux, µSv/y. The delivered preliminary near-field source term for BHA in Bq/year is shown in Appendix B.

It has been found recently that there is a possible discrepancy in the K_d values for Ra-226, Pb-210, and Po-210 since the recommended values used in both SR-Site (Crawford 2010) and SR-PSU (Crawford 2013) appear to give rise to unrealistic Po-210/Pb-210 activity ratios which are not

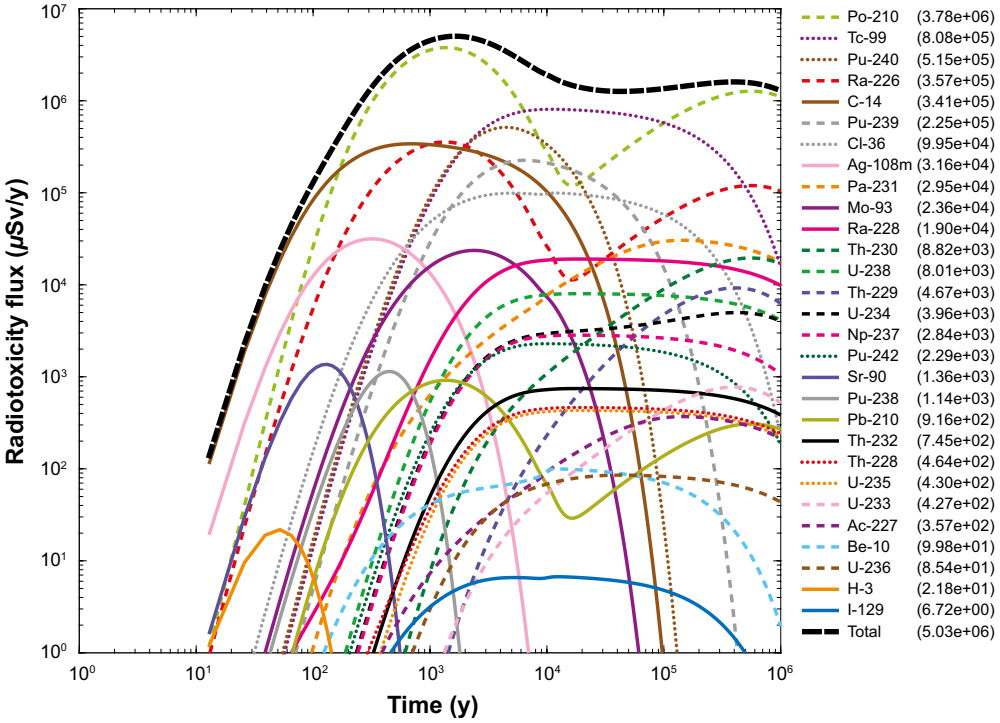

Figure 5-3. *Near-field source term for legacy waste (BHA) radiotoxicity as a function of time from release start. This is based on an early preliminary delivery. Radionuclides are listed in the legend in order of peak contribution to total radiotoxicity in the interval 0.1 ky–100 ky (units in μSv/y). Only radionuclides whose peak radiotoxicity contributes more than an equivalent fraction of 10^{-6} of the total peak source radiotoxicity are plotted.*

commensurate with typically occurring (natural analogue) groundwater levels. For this reason, in the present report it is assumed that the radioelements Pb, and Po be given the same K_d value as Ni to maintain dissolved activities approximately exhibiting secular equilibrium. This implies a decrease of the recommended K_d for Pb and an increase in the K_d for Po. It is noted that Ni was already invoked as a geochemical analogue of Pb in an SR-Site variant case (SKB 2010a) due to poor empirical data support for the Pb K_d value. It is acknowledged that the assumption of geochemical analogy of Pb with Ni is imperfect although it is expected to be approximately representative for groundwater with pH greater than about 8.5–9.0. The assumption may, however, underestimate K_d values for Pb at lower pH levels if biotite is deemed to be the primary sorbing phase.

The far-field breakthrough of various transported radionuclides is shown in Figure 5-4 for the reference case with original SR-PSU K_d values for Pb-210 and Po-210. Figure 5-5 shows the corresponding breakthrough with modified K_d values for Pb-210 and Po-210. As can be seen from Figure 5-4, the calculated breakthrough flux of Po-210 is, by far, the dose dominant nuclide for all times greater than about 0.1 ky and the transported radiotoxicity flux is calculated to be greater at the release point than the initial source term due to ingrowth of the Po-210 daughter from transported Ra-226 and Pb-210 along the migration path.

The very high values obtained for transported Po-210 radiotoxicity reflects the interplay between the relatively strong retardation of Pb-210 coupled with weak retardation of Po-210 giving a large accumulation of Po-210 in the aqueous phase. As noted above, this is clearly unrealistic when consideration is given to natural analogue data (see discussion of Po-210 in Crawford 2013). Use of the modified K_d values for Pb and Po raises the relative importance of Pb-210 and lowers the importance of Po-210 in the radiotoxicity breakthrough curve. The equivalent transported radiotoxicity of Po-210 and Pb-210 then track each other with mutual ratios characteristic of approximate secular equilibrium in the aqueous phase (taking into consideration the different dose conversion factors for each of the nuclides).

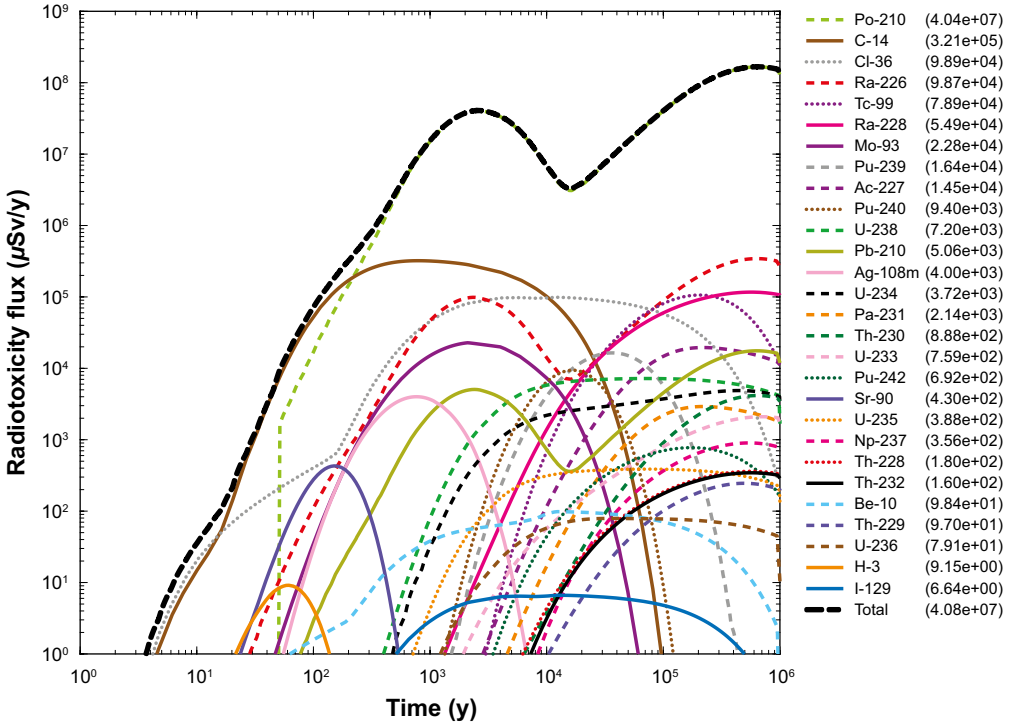

Figure 5-4. *Far-field breakthrough curves for transported legacy waste (BHA) radiotoxicity as a function of time (t_w = 6.4 y, $F = 5.4 \times 10^4$ y/m). Radionuclides are listed in the legend in order of peak contribution to total radiotoxicity in the interval 0.1 ky–100 ky (units in μSv/y) and assume the same K_d values for Po and Pb as in SR-Site. Only radionuclides whose peak radiotoxicity contributes more than an equivalent fraction of 10^{-6} of the total peak radiotoxicity are plotted.*

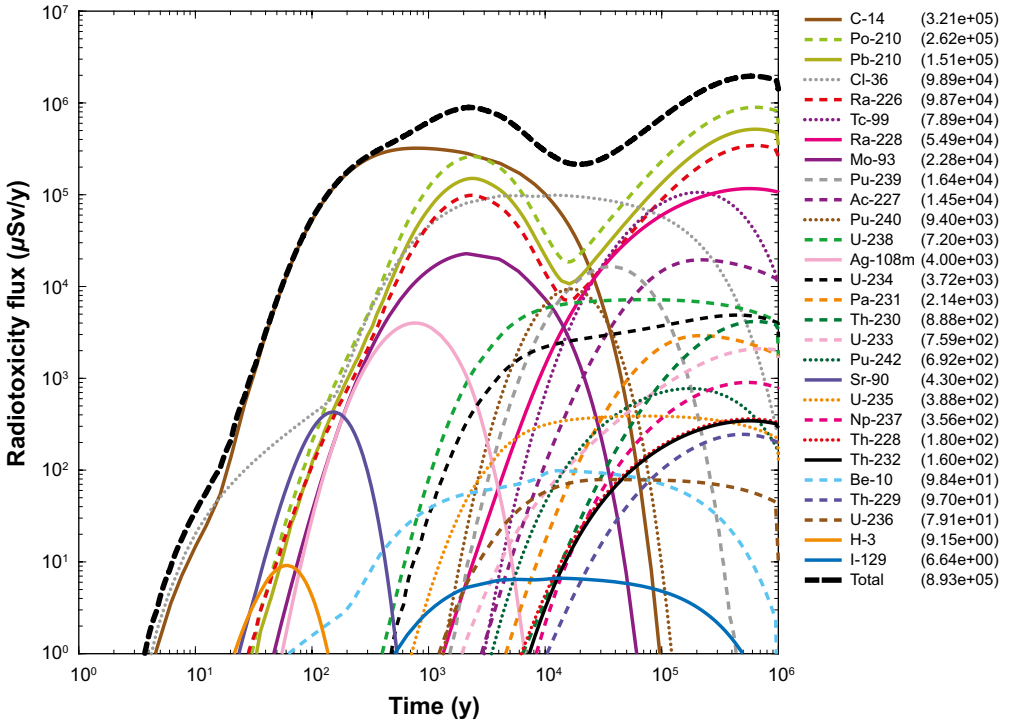

Figure 5-5. *Far-field breakthrough curves for transported legacy waste (BHA) radiotoxicity as a function of time (t_w = 6.4 y, $F = 5.4 \times 10^4$ y/m, revised K_d values for Pb, Po). Radionuclides are listed in the legend in order of peak contribution to total radiotoxicity in the interval 0.1 ky–100 ky (units in μSv/y). Only radionuclides whose peak radiotoxicity contributes more than an equivalent fraction of 10^{-6} of the total peak source radiotoxicity are plotted.*

Table 5-3 shows the results of the NuDec-Farf31 migration screening calculations for the legacy waste and various F-factors calculated in a similar fashion to those presented in the previous section. The top 10 potentially dose contributing nuclides are ordered in terms of their far-field peak dose contribution at any time in the time interval 0.1 ky–100 ky. The associated values are peak values of equivalent transported radiotoxicity expressed as a fraction of the total peak source radiotoxicity (Sv).

Table 5-3. Results of screening calculations indicating top 10 dose contributing nuclides for legacy wastes and various F-factors (using revised K_d values for Po and Pb) for the time interval 0.1 ky–100 ky. Values indicate the peak transported radiotoxicity expressed as a fraction of the total peak source radiotoxicity.

t_w	10 y		10 y		10 y		10 y
F-factor	10^3 y/m		10^4 y/m		10^5 y/m		10^6 y/m
Tc-99	1.47×10^{-1}	Po-210	1.30×10^{-1}	C-14	6.09×10^{-2}	C-14	3.11×10^{-2}
Po-210	9.30×10^{-2}	Tc-99	8.97×10^{-2}	Po-210	2.36×10^{-2}	Cl-36	1.74×10^{-2}
Pu-240	8.91×10^{-2}	Pb-210	7.53×10^{-2}	Cl-36	1.95×10^{-2}	Mo-93	2.99×10^{-3}
Ra-226	6.86×10^{-2}	C-14	6.70×10^{-2}	Pb-210	1.36×10^{-2}	Po-210	3.07×10^{-4}
C-14	6.76×10^{-2}	Ra-226	5.40×10^{-2}	Ra-226	9.41×10^{-3}	U-238	2.68×10^{-4}
Pb-210	5.55×10^{-2}	Pu-240	3.62×10^{-2}	Mo-93	4.42×10^{-3}	Pb-210	1.77×10^{-4}
Pu-239	4.11×10^{-2}	Ra-228	2.86×10^{-2}	Ra-228	2.90×10^{-3}	U-234	1.55×10^{-4}
Ac-227	2.08×10^{-2}	Pu-239	2.25×10^{-2}	Tc-99	2.56×10^{-3}	Ra-226	1.18×10^{-4}
Cl-36	1.98×10^{-2}	Ac-227	2.21×10^{-2}	U-238	1.34×10^{-3}	Be-10	1.69×10^{-5}
Ra-228	9.08×10^{-3}	Cl-36	1.98×10^{-2}	Pu-239	7.38×10^{-4}	U-235	1.58×10^{-5}

As can be seen from the screening calculations for legacy wastes, the long-lived actinides and their more short-lived progeny (many in secular equilibrium with parent nuclides) of the actinide chains dominate the contributions to transported far-field radiotoxicity for the legacy wastes. The nuclides from the radium ($4n+2$) chain, as well as Tc-99 are clearly very important in most of the F-factor scenarios tested. At the high end of the F-factor range, the actinides are more strongly attenuated and poorly sorbing nuclides become more prominent as might be expected.

6 Conclusions

6.1 Reactor (BHK) and Legacy (BHA) waste radionuclide inventories

This report details calculations that have been made in support of identifying a prioritised list of radionuclides for the SFL safety evaluation. Here, we also differentiate between the recommended list of nuclides necessary to adequately account for the evolution of radiotoxicity inventory over time and the list of dose dominant nuclides that are likely to have the largest impact on radiological safety performance measures. The minimum set of nuclides necessary to account for the time evolution of radiotoxicity is given in Table 4-1 and consists of 53 radionuclides. In this abbreviated set there are a number of converging chains explicitly defined. For radionuclide migration codes that cannot handle converging chains, the inventory of parent nuclides in the converging chains would need to be added to the daughter nuclide at the point of convergence, although this is only an approximate treatment over short to intermediate timescales.

Some additional non-chain and short-chain (non-actinide) fission and activation products in Table 4-1 could also be removed if the repository maintains its integrity over the first couple of hundred years. This concerns primarily the fast decaying radionuclides H-3, Eu-152, and to a lesser extent Sr-90. The radionuclide Sr-90, however, does persist in the inventory up until about 1 ky and is predicted to be very weakly retarded in migration calculations. Since it may be an important dose-determining nuclide for early arrival times it may not always be sensible for it to be excluded. An expanded list of nuclides is given in Table 6-2 which is based on the raw inventory data (see Section 3.1) together with a few additional nuclides not included in the inventory although explicitly accounted for in dose calculations via ingrowth.

It is difficult to identify a definitive ranked list of the most important dose determining nuclides since there are many assumptions implicit in the migration calculations used to make this judgement. Scoping transport calculations made using the Farf31 performance assessment code (via the interface program NuDec-Farf31) indicate that the dose dominant nuclides for the reactor wastes are primarily fission and activation products, while long-lived actinides and their progeny account for a large proportion of the dose dominant nuclides for the legacy wastes. In Table 6-2, an attempt has been made to identify those nuclides which regularly appear as top dose contributors in the screening calculations over a broad range of geosphere F-factors. These are color-coded in accordance with the key given in Table 6-1. The relative importance category assignment, however, is only indicative of the screening calculations made in this work and should be considered tentative.

The legacy wastes are generally more long-lived than the reactor wastes which is reflected in the evolution of total inventory radiotoxicity shown in Figure 4-6 to Figure 4-9. For the reactor wastes, the total radiotoxicity drops by nearly five orders of magnitude in the first 1 My simulated, whereas for the legacy wastes the total radiotoxicity only drops by about one order of magnitude over 1 My. The total radiotoxicity of the reactor waste (BHK) corresponds to roughly 5×10^7 Sv at closure, whereas for the legacy waste (BHA) the total radiotoxicity is about 1.3×10^7 Sv. In context, this roughly corresponds to about 20 % and 10 %, respectively of the total initial radiotoxicity inventory of a single BWR-I type spent fuel canister (SKB 2010d).

Table 6-1. Colour code explanation for screened radionuclides listed in Table 6-2.

Inventory status of nuclide – Reactor (BHK) or Legacy (BHA) waste	Color code
Nuclide explicitly accounted for in inventory	
Nuclide not present in inventory	
Nuclide not included in inventory, although explicitly accounted for in decay calculations	
Relative importance category	**Color code**
Short-lived nuclide only important at short times (≤ 1 ky) due to large inventory	
Important dose determining nuclide for intermediate to long timescales (1 ky–100 ky)	
Not significantly dose determining – possibly important (pulse release/chain ingrowth)	
Potentially dose determining nuclide strongly impacted by solubility limitation	
Insignificant dose contributor under most modelled situations in screening calculations	

Table 6-2. Summary of screening calculation results. See Table 6-1 for colour code explanations. Columns labelled BHK and BHA represent Reactor wastes and Legacy waste, respectively. Chain IDs are non-chain (N), short chain (S), thorium (4*n*), neptunium (4*n*+1), radium (4*n*+2), and actinium (4*n*+3) series. Very short lived non-ingrowing radionuclides ($t_{½}$ ≤ 10 y) or insignificant inventories (≤ 0.1 Sv total radiotoxicity) are highlighted with red bold text and in most cases can be reasonably neglected. Very short-lived decay-chain progeny implicitly included by assuming secular equilibrium are not tabulated in the inventory and are not included in this list.

Nuclide	Chain ID	Category	BHK	BHA	Nuclide	Chain ID	Category	BHK	BHA
H-3	N				**Eu-155**	N			
Be-10	N				Ho-166m	N			
C-14	N				**Ir-192**	N			
Na-22	N				Pb-210	4*n*+2			
Cl-36	N				Po-210	4*n*+2			
K-40	N				Ra-226	4*n*+2			
Ca-41	N				Ac-227	4*n*+3			
Fe-55	N				Ra-228	4*n*			
Ni-59	N				Th-228	4*n*			
Co-60	N				Th-229	4*n*+1			
Ni-63	N				Th-230	4*n*+2			
Se-79	N				Pa-231	4*n*+3			
Sr-90	S				Th-232	4*n*			
Mo-93	S				U-232	4*n*			
Nb-93m	S				U-233	4*n*+1			
Zr-93	S				U-234	4*n*+2			
Nb-94	N				U-235	4*n*+3			
Tc-99	S				U-236	4*n*			
Ru-106	S				Np-237	4*n*+1			
Pd-107	N				Pu-238	4*n*+2			
Ag-108m	N				U-238	4*n*+2			
Cd-113m	N				Pu-239	4*n*+3			
Sb-125	S				Pu-240	4*n*			
Sn-126	S				Am-241	4*n*+1			
I-129	N				Pu-241	4*n*+1			
Ba-133	S				Am-242m	4*n*+2			
Cs-134	N				Cm-242	4*n*+2			
Cs-135	N				Pu-242	4*n*+2			
Cs-137	S				Am-243	4*n*+3			
Pm-147	S				Cm-243	4*n*+3			
Sm-151	N				Cm-244	4*n*			
Eu-152	S				Cm-245	4*n*+1			
Eu-154	N				Cm-246	4*n*+2			

Note: I-129 in the reactor and legacy waste is a relatively insignificant dose contributor, although if released as an instantaneous pulse it might play a more prominent role.

6.2 Proposed list of prioritised radionuclides for SE-SFL

Based on the calculations made in previous sections and the selection criteria outlined in Chapter 4, a list of 65 unique radionuclides has been selected and are listed in Table 6-3 together with decay constants, references from which the decay constants are taken, and daughter radionuclides where applicable. C-14 is modelled separately as an inorganic-, induced-, and organic-fraction thereby giving a total of 67 modelled radionuclides. The set includes 58 radionuclides from the BHK and BHA wastes and 9 additional radionuclides unique to the ESS waste stream. It is noted that Co-60 is included in Table 6-3 even though it fails the selection criterion (i.e. short half-life < 10 y). This is because there is a relatively large radiotoxicity inventory initially present in the BHK waste (and to a lesser extent also in the BHA waste) and it is therefore considered an important "sentinel" radionuclide at short times even though it decays very rapidly to insignificant levels. Cs-135 is present in very low amounts (~109 mSv equivalent radiotoxicity), although is included anyway since it is a borderline case with regard to the radiotoxicity selection criteria. Pd-107 is also included on account of its very long half-life, even though present in insignificant amounts (0.2 mSv). All three of these were excluded from Table 4-1, however, on the grounds of being insignificant far-field dose contributors for all reasonable transport scenarios. Ar-39 is included here as an ESS-specific nuclide, although it is an inert gas and only present in very small amounts.

Table 6-3. List of radionuclides including all waste streams (BHK, BHA, and ESS-derived wastes) to be modelled in radionuclide transport calculations for SE-SFL. Decay constants and references are given for each radionuclide and daughter nuclides are indicated where applicable. Note that C-14 is modelled explicitly as an inorganic fraction, induced activity fraction, and organic fraction separately and therefore appears three times in the table giving a total of 67 nuclides.

Radionuclide	Decay constant (y^{-1})	Decay reference	Daughter
Ac-227	3.1840×10^{-2}	(Firestone et al. 1999)	
Ag-108m	1.5825×10^{-3}	(Schrader 2004)	
Am-241	1.6038×10^{-3}	(Firestone et al. 1999)	Np-237
Am-242m	4.9159×10^{-3}	(Firestone et al. 1999)	Cm-242
Am-243	9.4050×10^{-5}	(Firestone et al. 1999)	Pu-239
Ar-39	2.5768×10^{-3}	ICRP 2008, Annex A, Table A.1	
Ba-133	6.5951×10^{-2}	(Firestone et al. 1999)	
Be-10	4.5904×10^{-7}	(Firestone et al. 1999)	
Ca-41	6.7296×10^{-6}	(Firestone et al. 1999)	
Cd-113m	4.9159×10^{-2}	(Firestone et al. 1999)	
C-ind-14	1.2097×10^{-4}	(Firestone et al. 1999)	
C-inorg-14	1.2097×10^{-4}	(Firestone et al. 1999)	
Cl-36	2.3028×10^{-6}	(Firestone et al. 1999)	
Cm-242	1.5541×10^{-0}	(Firestone et al. 1999)	Pu-238
Cm-243	2.3819×10^{-2}	(Firestone et al. 1999)	Pu-239
Cm-244	3.8295×10^{-2}	(Firestone et al. 1999)	Pu-240
Cm-245	8.1547×10^{-5}	(Firestone et al. 1999)	Pu-241
Cm-246	1.4654×10^{-4}	(Firestone et al. 1999)	Pu-242
Co-60	1.3149×10^{-1}	(Firestone et al. 1999)	
C-org-14	1.2097×10^{-4}	(Firestone et al. 1999)	
Cs-135	3.0137×10^{-7}	(Firestone et al. 1999)	
Cs-137	2.3051×10^{-2}	(Firestone et al. 1999)	
Eu-150	1.8784×10^{-2}	ICRP 2008, Annex A, Table A.1	
Eu-152	5.1204×10^{-2}	(Firestone et al. 1999)	
Gd-148	9.2915×10^{-3}	ICRP 2008, Annex A, Table A.1	
H-3	5.6216×10^{-2}	(Firestone et al. 1999)	
Ho-166m	5.7762×10^{-4}	(Firestone et al. 1999)	
I-129	4.4150×10^{-8}	(Firestone et al. 1999)	
K-40	5.4279×10^{-10}	ICRP 2008, Annex A, Table A.1	
La-137	1.1552×10^{-5}	ICRP 2008, Annex A, Table A.1	
Mo-93	1.7329×10^{-4}	(Firestone et al. 1999)	Nb-93m
Nb-93m	4.2973×10^{-2}	(Firestone et al. 1999)	
Nb-94	3.4145×10^{-5}	(Firestone et al. 1999)	

Radionuclide	Decay constant (y^{-1})	Decay reference	Daughter
Ni-59	9.1204×10^{-6}	(Firestone et al. 1999)	
Ni-63	6.9245×10^{-3}	(Firestone et al. 1999)	
Np-237	3.2330×10^{-7}	(Firestone et al. 1999)	U-233
Pa-231	2.1155×10^{-5}	(Firestone et al. 1999)	Ac-227
Pb-210	3.1083×10^{-2}	(Firestone et al. 1999)	Po-210
Pd-107	1.0664×10^{-7}	(Firestone et al. 1999)	
Po-210	1.8289×10^{0}	(Firestone et al. 1999)	
Pu-238	7.9036×10^{-3}	(Firestone et al. 1999)	U-234
Pu-239	2.8749×10^{-5}	(Firestone et al. 1999)	U-235
Pu-240	1.0561×10^{-4}	(Firestone et al. 1999)	U-236
Pu-241	4.8303×10^{-2}	(Firestone et al. 1999)	Am-241
Pu-242	1.8568×10^{-6}	(Firestone et al. 1999)	U-238
Ra-226	4.3322×10^{-4}	(Firestone et al. 1999)	Pb-210
Ra-228	1.2055×10^{-1}	(Firestone et al. 1999)	Th-228
Re-186m	3.4657×10^{-6}	ICRP 2008, Annex A, Table F.1	
Se-79	2.1197×10^{-6}	(Firestone et al. 1999)	
Si-32	5.2511×10^{-3}	ICRP 2008, Annex A, Table A.1	
Sm-151	7.7016×10^{-3}	(Firestone et al. 1999)	
Sr-90	2.4084×10^{-2}	(Firestone et al. 1999)	
Tb-157	9.7626×10^{-3}	ICRP 2008, Annex A, Table A.1	
Tb-158	3.8508×10^{-3}	ICRP 2008, Annex A, Table A.1	
Tc-99	3.2835×10^{-6}	(Firestone et al. 1999)	
Th-228	3.6290×10^{-1}	(Firestone et al. 1999)	
Th-229	9.4447×10^{-5}	ICRP 2008, Annex A, Table A.1	
Th-230	9.1946×10^{-6}	(Firestone et al. 1999)	Ra-226
Th-232	4.9511×10^{-11}	(Firestone et al. 1999)	Ra-228
Ti-44	1.1552×10^{-2}	ICRP 2008, Annex A, Table A.1	
U-232	1.0060×10^{-2}	(Firestone et al. 1999)	Th-228
U-233	4.3539×10^{-6}	(Firestone et al. 1999)	Th-229
U-234	2.8234×10^{-6}	(Firestone et al. 1999)	Th-230
U-235	9.8486×10^{-10}	(Firestone et al. 1999)	Pa-231
U-236	2.9596×10^{-8}	(Firestone et al. 1999)	Th-232
U-238	1.5514×10^{-10}	(Firestone et al. 1999)	U-234
Zr-93	4.5304×10^{-7}	(Firestone et al. 1999)	Nb-93m

References

SKB's (Svensk Kärnbränslehantering AB) publications can be found at www.skb.com/publications. SKBdoc documents will be submitted upon request to document@skb.se.

Bateman H, 1910. The solution of a system of differential equations occurring in the theory of radioactive transformations. Proceedings of the Cambridge Philosophical Society 15, 423–427.

Crawford J, 2010. Bedrock K_d data and uncertainty assessment for application in SR-Site geosphere transport calculations. SKB R-10-48, Svensk Kärnbränslehantering AB.

Crawford J, 2013. Quantification of rock matrix K_d data and uncertainties for SR-PSU. SKB Report R-13-38, Svensk Kärnbränslehantering AB.

Crawford J, Löfgren M, 2018. Modelling of radionuclide retention by matrix diffusion in a layered rock model. SKB R-17-22, Svensk Kärnbränslehantering AB.

Elfwing M, Evins L Z, Gontier M, Grahm P, Mårtensson P, Tunbrant S, 2013. SFL concept study. Main report. SKB TR-13-14, Svensk Kärnbränslehantering AB.

EPA, 1993. External exposure to radionuclides in air, water, and soil. Federal Guidance Report No. 12, EPA-402-R-93-081, Oak Ridge National Laboratory, Oak Ridge, TN; US Environmental Protection Agency, Washington, DC.

EU, 1996. Council Directive 96/92/EURATOM of 13 May 1996 laying down basic safety standards for the protection of the health of workers and the general public against the dangers arising from ionizing radiation. Luxembourg: European Commission.

Firestone R, Baglin C (ed), Chu S (ed), 1999. Table of isotopes: 1999 update. 8th ed. New York: Wiley.

Herschend B, 2014. Long-lived intermediate level waste from Swedish nuclear power plants. Reference Inventory. SKB R-13-17, Svensk Kärnbränslehantering AB.

ICRP, 1995. Age-dependent doses to the members of the public from intake of radionuclides – Part 5 Compilation of ingestion and inhalation coefficients. Oxford: Pergamon. (ICRP Publication 72; Annals of the ICRP 26(1))

ICRP, 2008. Nuclear decay data for dosimetric calculations. Oxford: Pergamon. (ICRP Publication 107; Annals of the ICRP 38 (3))

ICRP, 2012. Compendium of dose coefficients based on ICRP Publication 60. Oxford: Pergamon. (ICRP Publication 119; Annals of the ICRP 41 (Suppl.))

Jörg G, Bühnemann R, Hollas S, Kivel N, Kossert K, Van Winckel S, Gostomski C L, 2010. Preparation of radiochemically pure ^{79}Se and highly precise determination of its half-life. Applied Radiation and Isotopes 68, 2339–2351.

Lindgren M, Gylling B, Elert M, 2002. Säkerhet och Vetenskap. FARF31 Version 1.2. User's guide. Arbetsrapport TS-02-03, Svensk Kärnbränslehantering AB.

Moral L, Pacheco A F, 2003. Algebraic approach to the radioactive decay equations. American Journal of Physics 71, 684–686.

Norman S, Kjellbert N, 1990. FARF31 – A far field radionuclide migration code for use with the PROPER package. SKB TR 90-01, Svensk Kärnbränslehantering AB.

Schrader H, 2004. Half-life measurements with ionization chambers – a study of systematic effects and results. Applied Radiation and Isotopes 60, 317–323.

SKB, 2010a. Radionuclide transport report for the safety assessment SR-Site. SKB TR-10-50, Svensk Kärnbränslehantering AB.

SKB, 2010b. Data report for the safety assessment SR-Site. SKB TR-10-52, Svensk Kärnbränslehantering AB.

SKB, 2010c. Comparative analysis of safety related site characteristics. SKB TR-10-54, Svensk Kärnbränslehantering AB.

SKB, 2010d. Spent nuclear fuel for disposal in the KBS-3 repository. SKB TR-10-13, Svensk Kärnbränslehantering AB.

SKB, 2014. Data report for the safety assessment SR-PSU. SKB TR-14-10, Svensk Kärnbränslehantering AB.

SKB, 2015. Radionuclide transport and dose calculations for the safety assessment SR-PSU. Revised edition. SKB TR-14-09, Svensk Kärnbränslehantering AB.

Thomson G, Miller A, Smith G, Jackson D, 2008. Radionuclide release calculations for SAR-08. SKB R-08-14, Svensk Kärnbränslehantering AB.

Appendix A

The NuDec-Inventory program

Background

For a number of years, the DECAY program developed as an in-house tool at Kemakta Konsult AB has been used in a supporting role for radionuclide inventory calculations within various SKB projects. It has mostly been used for scoping calculations and preparing explanatory report and presentation graphics and has not been used directly in a quantitative role for safety assessment calculations (and therefore is not specifically cited in the historical safety assessments). Recently, the present author created a new software tool within Matlab to take over this role with greater flexibility for producing report graphics and scoping calculations of the type described in this report. From a QA perspective, there are also clear advantages to using a procedural script-based code with clearly defined and archivable input and output files and transparent numerical procedures unlike DECAY, which is based on an externally compiled Fortran program called from within a MS Excel 4.0 macro function. The impetus to develop an alternative to this software tool was also driven by the fact that the original code no longer functions on modern 64-bit MS Windows machines and would require some development work to properly modernise.

The NuDec-Inventory code forms part of the NuDec code family currently in development. This is a set of three separate codes intended for making simplified and fast scoping calculations integrating the calculation of radionuclide inventories, near-field release (source term), and far-field migration simulations. NuDec consists of three core components:

- **NuDec-Inventory**
- **NuDec-Source**
- **NuDec-Farf31**

The NuDec-Source program is in an early stage of prototype development and since it is not used in this work, will not be discussed further in this report. It will be reported in a later project, however, if deemed to be a useful tool. The NuDec-Farf31 code for geosphere migration calculations is used extensively in this work, although results are only used to provide context in support of the selection of prioritised radionuclides. NuDec-Farf31 is based on the Farf31 code together with a Matlab script interface to streamline input and outputs and to produce report and presentation graphics. The tool is described more fully in Crawford and Löfgren (2018) where it is used to replicate the central corrosion case from SR-Site. The selection of prioritised radionuclides discussed in this work is based solely on the simulated evolution of total radionuclide inventory over time assuming no depletion of the inventory due to migration processes. The following section describes the NuDec-Inventory code which is used extensively in the work described in this report.

Description of the NuDec-Inventory code

NuDec-Inventory consists of two sub-units; a simple radionuclide database management tool and a main calculation program. These are described in the following sections.

Database management tool

The database management program reads in three TAB-delimited files:

1. nuclide_data.dat
2. dose_factor_data.dat
3. element_Kd_data.dat

The “nuclide_data.dat” input file contains decay chain definitions and other data necessary to calculate the evolution of radionuclide inventory over time. The data fields contained in this input file are described in Table A-1.

Table A-1. Data fields contained in the nuclide_data.dat input file. Blank field entries are signified by the "null" text string to preserve the column structure in the input file.

Variable	Description
chain_id	identifying code for decay chain: −1 = single nuclide (no active product) 0 = 4*n* decay series 1 = 4*n* + 1 decay series 2 = 4*n* + 2 decay series 3 = 4*n* + 3 decay series 4 = short chain decay process (non-actinide)
atomic_number	atomic number of decaying radionuclide
atomic_weight	atomic weight of decaying radionuclide
isomer	isomer identifying code (values: null, m, m^2)
nuclide	radionuclide name (e.g. U-234)
t50	half-life (units specified by *time_unit* field)
sigma_t50	half-life uncertainty (units specified by *time_unit* field)
time_unit	half-life time units, possibilities are: y = years d = days h = hours m = minutes s = seconds
t_conv_factor	time unit conversion factor *time_unit* to y
t50_y	half-life (y)
sigma_t50_y	half-life uncertainty (y)
alpha	α-decay energy (MeV)
beta	β-decay energy (MeV)
gamma	γ-decay energy (MeV)
progeny	number of daughter radionuclides
daughter_1	daughter #1 radionuclide name (e.g. Th-230)
fraction_1	decay fraction #1
daughter_2	daughter #2 radionuclide name
fraction_2	decay fraction #2

This is essentially the same database structure used in the original DECAY program with some minor additions and deletions. It can be easily edited in MS Excel and saved by exporting to a tab-delimited file format which can be read by the database management tool. Radionuclide half-lives were updated in the database in accordance with the description previously given in Section 3.1. The second input file contains dose factors for conversion of radionuclide activity (Bq) to radiotoxicity (Sv). Different versions of this file have been used in different projects according to the particular requirements of the project. The default data file is a tab-delimited version of ingestion dose factors taken directly from Table F.1 in ICRP (2012). For the SE-SFL project, however, a MS Excel data file was provided by SKB containing external air exposure dose factors (EPA 1993), ingestion dose factors and inhalation exposure dose factors (ICRP 1995) for the set of 67 radionuclides specified in Table 6-3. This was converted to a single text file in tab-delimited format and used as the "dose_factor_data.dat" input file. Data fields for this input file are defined in Table A-2.

Table A-2. Data fields contained in the dose_factor_data.dat input file for the SE-SFl project. Blank field entries are signified by the "null" text string to preserve the column structure in the input file. Since induced, organic, and inorganic forms of C-14 were deemed to have the same dose conversion factors, field four (nuclide_form) may be considered redundant for the purposes of the present project, although it is included for backward code compatibility.

Variable	Description
atomic_number	atomic number of radionuclide
atomic_weight	atomic weight of decaying radionuclide
isomer	isomer identifying code (values: null, m, m^2)
nuclide_form	specific form of radionuclide, possibilities are: all = all forms ind = induced activity (C-14) org = organic form (C-14) inorg = inorganic form (C-14)
doseCoef_ing	ingestion exposure dose coefficient ($Sv \times Bq^{-1}$)
doseCoef_ext	external exposure dose coefficient $(Sv \times h^{-1})/(Bq \times m^{-3})$
doseCoef_inh	inhalation exposure dose coefficient ($Sv \times Bq^{-1}$)

The third input file "element_Kd_data.dat" contains K_d data for transport calculations using NuDec-Farf31. This data file contains several columns of data with site specific K_d values used in SR-Site for Forsmark (SKB 2010b) and Laxemar (SKB 2010c) as well as SR-PSU (SKB 2014). This data is only used by NuDec-Farf31 and site-specific values can be selected by the user when running the program. NuDec-Farf31 also allows the user to redefine individual K_d values for what-if calculations (at run-time) if required without making changes to the archived database. For SE-SFL, K_d values for the SR-Site Laxemar site comparison case (SKB 2010c) were mostly used with some additions taken from Crawford (2013) and new radionuclides not previously considered previously were conservatively assigned K_d values of zero.

The database management program reads all three input data files and stores copies as Matlab struct-type variables which are stored in a database file in the Matlab ".mat" binary format. These data are then loaded and used as needed by the NuDec-Inventory and NuDec-Farf31 codes at run-time. The database file is saved with the filename "nuclide_database_YYYY-MM-DD.mat" where "YYYY-MM-DD" is the date on which the database file was generated. The inclusion of the creation date in the filename was considered important for transparency and QA reasons since values for specific input data fields can be revised throughout a project.

The most important function of this program, however, is the creation of a global $(n \times n)$ decay matrix (A) where n is the number of radionuclides defined in the "nuclide_data.dat" input file. This matrix contains all the dependencies between different radionuclides in the various decay chains. It is assembled by combining the decay rates of each parent radionuclide (diagonal entries) with the corresponding (off-diagonal entries) for progeny ingrowth terms including stochastic split fractions where there are multiple daughters from a given parent radionuclide. The matrix assembly is achieved by a simple text string search and indexing procedure which is used to create a list of row and column indices for progeny ingrowth processes. The list of row and column indices is then used to define the sparse A-matrix which is saved in the database file and is used directly in the solution procedure described in the next section. The code procedure used to create the A-matrix is shown in Table A-4.

Table A-3. Data fields contained in the element_Kd_data.dat input file for the SE-SFL project. Blank field entries are signified by the "null" text string to preserve the column structure in the input file.

Variable	Description
element	Name of radioelement (e.g. U, Ni, etc.)
atomic_number	Atomic number of radioelement
Kd_PSU	K_d value (m^3/kg), SR-PSU
Kd_Fm	K_d value (m^3/kg), SR-Site Forsmark
Kd_Lx	K_d value (m^3/kg), SR-Site Laxemar

Table A-4. String search and indexing procedure used to calculate the A-matrix (referred to as the symbol "lambda" in the Matlab code extract below). The database is read as a tab-delimited file and stored as a Matlab struct variable (symbol "nuclide_data") where the fields correspond to the variable names listed in Table A-2.

```
% import radionuclide database as tab-delimited file
nuclide_data = tdfread(['nuclide_data.dat'],'\t');

% get name list of all nuclides
names = nuclide_data.nuclide;

% calculate decay rate constants (1/y) of nuclides
t_half = nuclide_data.t50_y;
k = log(2)./t_half;
nn = length(k);

% find first daughters
dnam = nuclide_data.daughter_1;
frac = nuclide_data.fraction_1;
dnam_idx = zeros(nn,1);
for i = 1:nn
    mask = strcmp(deblank(dnam(i,:)),cellstr(names));
    if nnz(mask) > 0
        dnam_idx(i) = find(mask);
    end
end
ix = find(dnam_idx);
node_list = [dnam_idx(ix),ix];
frac_list = frac(ix);
node_name_list = [names(ix,:),dnam(ix,:)];

% find second daughters
dnam = nuclide_data.daughter_2;
frac = nuclide_data.fraction_2;
dnam_idx = zeros(nn,1);
for i = 1:nn
    mask = strcmp(deblank(dnam(i,:)),cellstr(names));
    if nnz(mask) > 0
        dnam_idx(i) = find(mask);
    end
end
ix = find(dnam_idx);
node_list = [node_list;[dnam_idx(ix),ix]];
frac_list = [frac_list;frac(ix)];
node_name_list = [node_name_list;[names(ix,:),dnam(ix,:)]];

%% assemble lambda matrix

% define diagonals
lambda = spdiags(-k,0,speye(nn,nn));

% define off-diagonal entries
ix = node_list(:,1);
iy = node_list(:,2);
arg = k(iy).*frac_list;
lambda_od = sparse(ix,iy,arg,nn,nn);
lambda = lambda + lambda_od;
```

NuDec-Inventory main program

The original DECAY program was based on a full numerical solution of the decay chain ordinary differential equations using a stiff ODE solver:

$$\frac{d\overline{c}}{dt} = A\,\overline{c} \tag{A-1}$$

Where, elements of the radionuclide concentration vector $\overline{c}$ are related to the activity vector $\overline{a}$ by:

$$c_i = \frac{a_i}{N_{av} k_i} \qquad\qquad k_i(\mathrm{s}^{-1}) = \frac{\ln(2)}{t_{½}} \tag{A-2}$$

Here, k_i (s^{-1}) is the decay constant, N_{av} (mol^{-1}) is Avogadro's constant, and $t_{½}$(s) is the half-life of the radionuclide. The global decay constant array, A is defined by the database management tool and includes all radionuclides present in the archived database. The NuDec-Inventory program, rather than directly solving the ordinary differential Equation A-1, makes use of the matrix algebraic solution described by (Moral and Pacheco 2003):

$$\overline{c} = V \Lambda V^{-1} \overline{c}_0 \tag{A-3}$$

Where, Λ is the $n \times n$ diagonal matrix,

$$\Lambda = \mathrm{diag}\left(\exp\left(-\Lambda_j t\right)\right) \qquad\qquad \forall\, \Lambda_j : j = 1,\ldots,n \tag{A-4}$$

The, Λ_j parameters in Equation A-4 are the eigenvalues of the A-matrix, while V is the matrix of eigenvectors of A:

$$V = \left(\overline{v}_1 \middle| \overline{v}_2 \middle| \cdots \middle| \overline{v}_n\right) \tag{A-5}$$

Whose columns (eigenvectors) are defined by:

$$A\overline{v}_i = \Lambda_i \overline{v}_i \qquad\qquad i = 1,\ldots,n \tag{A-6}$$

Being based on an eigenvector approach, the solution given by Equation A-3 is subject to the same restriction as the Bateman equation method (Bateman 1910); namely that no two decay processes are permitted to have the same decay constant since this is a requirement for the A-matrix to be non-singular and diagonalisable. This assumption is generally fulfilled for most decay chains of interest in radioactive waste management and can be readily verified by examining the half-lives of radionuclides included in the database. If the assumption is violated, the numerical evaluation will also return an error for matrix singularity and such a condition is therefore easily identified. The above-described solution for the time-dependent evolution of the radionuclide concentration vector can be compactly written in five lines of Matlab script as shown in Table A-5.

Table A-5. Solution procedure for solving the time dependent evolution of radionuclide concentrations given the A-matrix (here referred to by the symbol "lambda", assembled in sparse matrix form by the database management tool described in the previous section), and the vector of requested output times (symbol "tt").

```
[V,D] = eig(full(lambda));
for i = 1:numel(tt)
    big_lambda = diag(exp(diag(D)*tt(i)));
    c(i,:) = [V*big_lambda*inv(V)*c0]';
end
```

As can be appreciated from this code snippet, there are no user supplied functions or subroutines and all operations are defined in terms of well-validated Matlab core functions. In this code representation, symbol "V" corresponds to the eigenvector matrix (Equation A-5) and "D" is the associated column vector of eigenvalues, which together with the time is used to calculate "big_lambda" which is the symbol representing diagonal matrix Λ (Equation A-4). The symbol "c0" represents the initial radionuclide concentration and the columns of array "c" then correspond to the radionuclide concentrations at each requested output time, t_i. The radionuclide activity as a function of time is then obtained by using the rearranged version of Equation A-2 to convert from concentration to activity. The code has been tested against the result obtained using the original MS Excel DECAY macro program for the case of the U-238 decay chain (initially 1 MBq U-238 and 10^{-6} Bq for all daughter nuclides) and agree to a relatively high degree of precision. The results of this comparison are shown in Figure A-1.

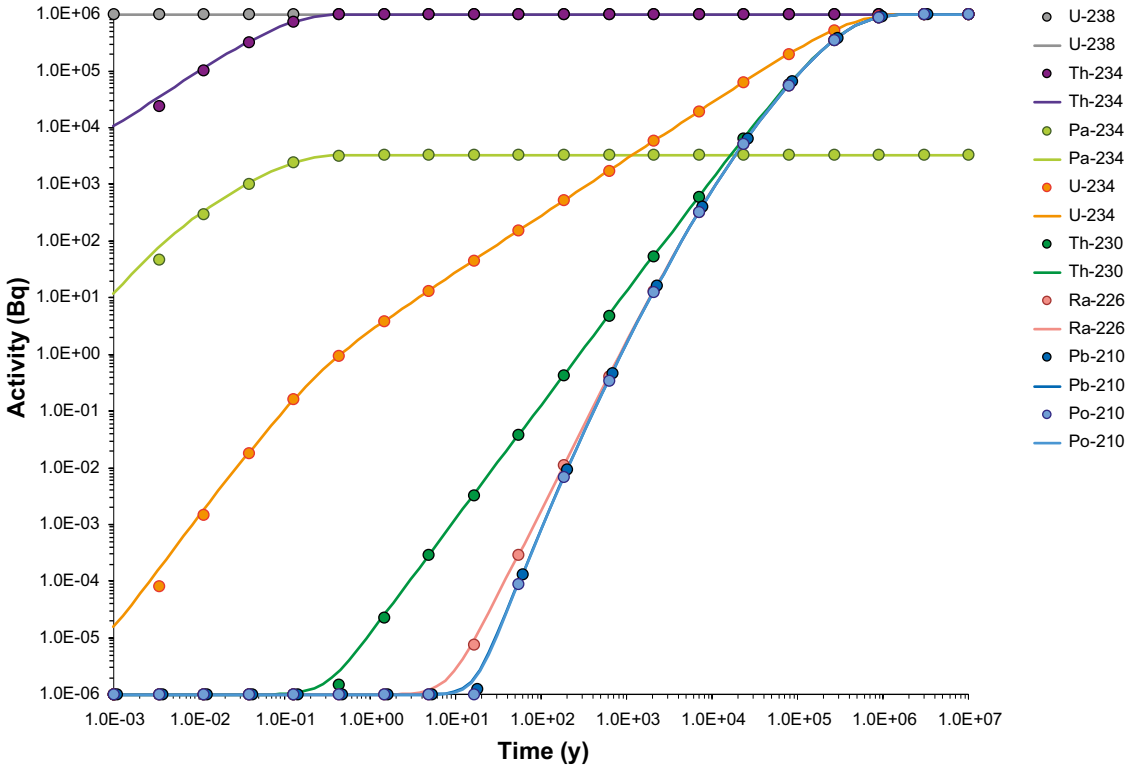

Figure A-1. *Comparison between the calculation results of the DECAY program (circular markers) calculated in MS Excel and the results calculated by NuDec-Inventory (unbroken curves) for the U-238 decay chain assuming an initial inventory activity of 1 MBq U-238 and 10^{-6} Bq for all daughter nuclides in the chain.*

Appendix B

Near-Field Source Term used in Transport Calculations

For the transport calculations made using Farf31 (via the NuDec-Farf31 interface), a near-field source term has been assumed. This was based on an early data set provided by SKB in the form of two Microsoft Excel files; one for BHK and one for BHA, respectively. These dat files contain data values given in Bq/y for 10 000 logarithmically-spaced time points between the start year (2075 AD) and 1 Ma. The near-field activity flux tabulated in these data files is plotted in Figure B-1 for BHK, and in Figure B-2 for BHA in units of MBq/y. Only radionuclides contributing more than 1 Bq/y are plotted in the figures.

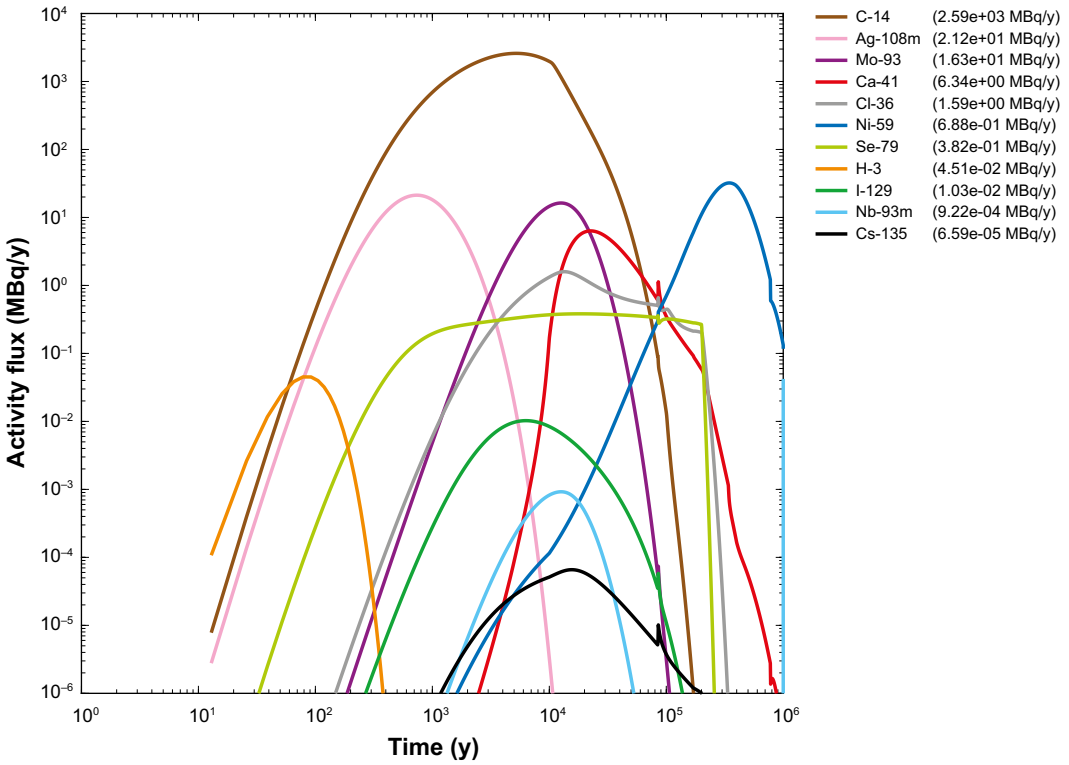

Figure B-1. *Near-field source term for reactor waste (BHK) activity flux (MBq/y) as a function of time from release start (2075 AD). This is based on an early preliminary data delivery. Radionuclides are listed in the legend in order of peak contribution to total activity flux in the interval 0.1 ky- 100 ky (units in MBq/y). Only radionuclides contributing more than 1 Bq/y are plotted.*

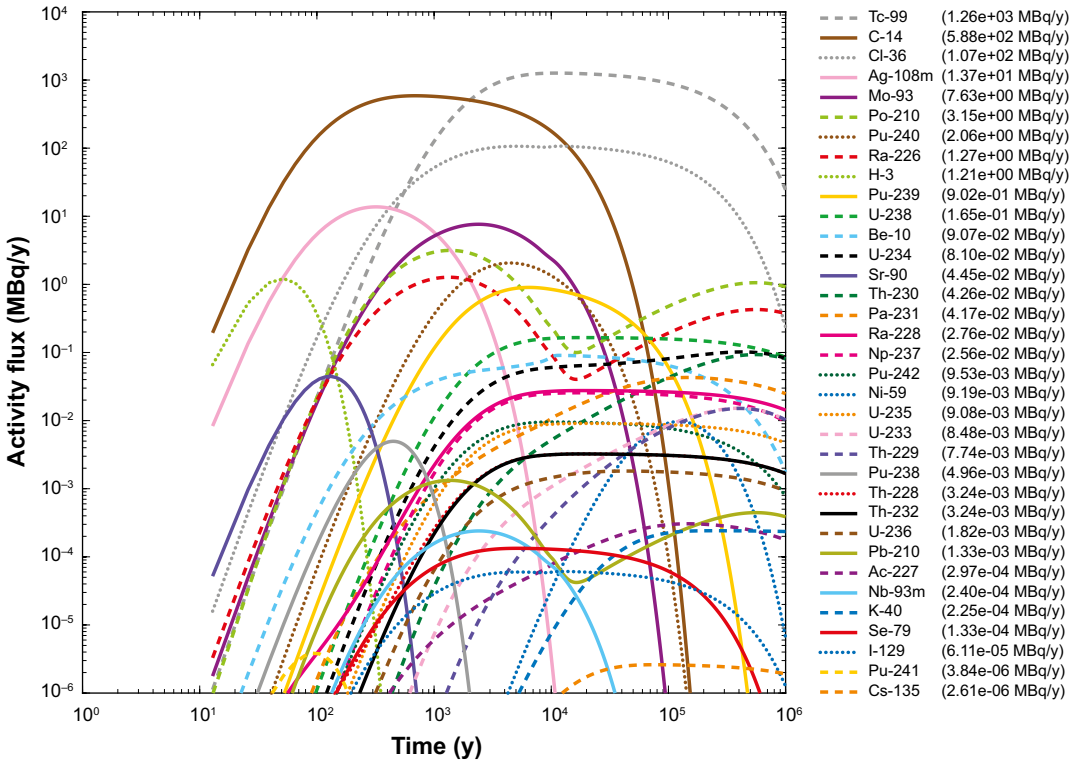

Figure B-2. *Near-field source term for legacy waste (BHA) activity flux (MBq/y) as a function of time from release start (2075 AD). This is based on an early preliminary data delivery. Radionuclides are listed in the legend in order of peak contribution to total activity flux in the interval 0.1 ky- 100 ky (units in MBq/y). Only radionuclides contributing more than 1 Bq/y are plotted.*

Arkitektkopia AB, Bromma, 2019

SKB is responsible for managing spent nuclear fuel and radioactive waste produced by the Swedish nuclear power plants such that man and the environment are protected in the near and distant future.

skb.se